Yiğit Şener, BSc

An acoustic particle velocity sensor using a plasma: a feasibility study

Master's Thesis

to achieve the university degree of

Master of Science

Master's degree programme: Mechanical Engineering and Business Economics

Submitted to

Graz University of Technology

Executed at

Supervisor

Univ. Prof. iR DI. Dr. Hans H. Priebsch

Institute of Internal Combustion Engines and Thermodynamics, Graz University of Technology

Supervisor

Priv.-Doz. Dipl.-Ing. Dr.techn. Anton Fuchs

Institute of Electrical Measurement and Measurement Signal Processing, Graz University of Technology

Supervisor

MSc. Eugene Nijman

Virtual Vehicle Research GmbH, Graz

Graz, February 2020

Institut für Verbrennungskraftmaschinen und Thermodynamik
Vorstand: Univ.-Prof. DI Dr. Helmut Eichlseder

Acknowledgements

Firstly, I would like to share my gratitude with my family. They have been supporting me through my master study no matter what I choose to do. I also thank my friends who have been supporting me and being by my side all the time. Mr. Eugene Nijman, my supervisor at the Virtual Vehicle Research GmbH Research Centre, guided me from the beginning of my thesis work. With his support, it was possible to write this thesis with great challenges from various fields such as acoustics, plasma physics and electronics. Thanks to my supervisor at the Technical University of Graz, Prof. Hans-Herwig Priebsch, I could adapt my approach to various technical difficulties and bring consistent results. In this context, I would like to thank also Dr. Christopher Albert at Max Planck Institute of Plasma Physics who has supported me to understand the concept of plasma and plasma conductivity. Moreover, I wish to show my gratitude to Dr. Jan Rejlek, who has assisted me through my thesis. Finally, I would like to pay my special regards to Priv.-Doz. Anton Fuchs at the Technical University of Graz who has given me the opportunity to work in this interesting research.

The Master thesis was written at VIRTUAL VEHICLE Research GmbH in Graz, Austria. The authors would like to acknowledge the financial support of the COMET K2 – Competence Centers for Excellent Technologies Programme of the Federal Ministry for Transport, Innovation and Technology (bmvit), the Federal Ministry for Digital and Economic Affairs (bmdw), the Austrian Research Promotion Agency (FFG), the Province of Styria and the Styrian Business Promotion Agency (SFG).

Affidavit

I declare that I have authored this thesis independently, that I have not used other than the declared sources/resources, and that I have explicitly indicated all material which has been quoted either literally or by content from the sources used. The text document uploaded to TUGRAZonline is identical to the present Master's thesis.

_____	_____
Date	Signature

Abstract

In automotive, acoustics is a measure of quality and fineness of the product. Therefore, manufacturers put a lot of effort to make the best possible acoustic refinement on their vehicles, which depend on computer simulations and experiments. Nowadays, a variety of acoustic simulations can be made with specially developed software for automotive use. However, experimental methods are still more dependable and are widely used to investigate the acoustic characteristics of vehicles. Among those methods, sound intensity measurements in the near field play a significant role in providing data to generate sound intensity maps in which sound propagation direction with its magnitude can be illustrated. Thanks to the sound intensity map one can detect multiple sound sources and prioritize the problematic regions to treat. Sound intensity measurement is done by combining sound pressure and acoustic particle velocity data by an intensity probe. Obtaining acoustic particle velocity here illustrates a more significant challenge than sound pressure measurement. There are several commercially available methods to determine particle velocity. For all those methods significant limitations occur. Thus, their application range is restricted in testing. The goal of this research is to search for a new technique that can provide an advantage for detecting the sound characteristics of vehicles in the near field. Specifically, higher accuracy and easy calibration of the measurement device would be a breakthrough in sound intensity measurements. In this master's thesis, a novel method to determine particle velocity and its feasibility are introduced. The novelty of this method is that plasma is used to make air electrically conductive for the measurement.

The structure of the thesis is outlined as follows. Initially, the definition of sound intensity and particle velocity is treated with the presentation of different methods to measure. Those measurement methods are thoroughly investigated in two main groups and corresponding advantages and disadvantages are discussed. Afterwards, the concept of novel particle velocity measurement is introduced following an explanation of the measurement principles. In chapter 3, where the theory is explained, the concept of plasma and relevant parameters for this research are investigated. The outcome of those investigations are compared with relevant boundary conditions for discussion of feasibility Eventually, design of measurement setup is introduced that is made of commercially available parts in chapter 4. Consequently, the feasibility of the measurement method is presented at the end of the thesis.

List of Abbreviations

a	Acceleration (m/s^2)
A_D	Differential gain of the amplifier (-)
APPJ	Air pressure plasma jet
B	Magnetic flux density (T)
$\vec{B}$	Magnetic flux density vector (T)
d	Drift region
D	Doppler shift (m^{-1})
DBD	Dielectric barrier discharge
e	Electron charge (C)
$\vec{E}$	Electric field (V/m)
F	Force (N)
F_B	Bragg cell frequency (Hz)
$\overrightarrow{F_C}$	Coulomb force (N)
F_D	Doppler frequency (Hz)
$\overrightarrow{F_L}$	Lorentz Force (N)
i	Wavelength of reflected light (m)
I	Current (A)
$\vec{I}$	Sound intensity vector (W/m^2)
k	Ratio of specific heats (-)
k_B	Boltzmann constant (J/K)
L	Distance between electrodes (m)
LDA	Laser Doppler anemometry
m	Mass (kg)
n	Charge density (m^{-3})
p	Sound pressure (Pa)
P	Sound power (W)
PDD	Piezoelectric direct discharge
PPVS	Plasma particle velocity sensor
PZT	Piezoelectric transducer
q	Average transport cross section of electrons (m^2)
QD	Quadrature demodulation
r_O	Impact parameter (m)

R	Resistance (Ω)
$\vec{S}$	Area vector (m^2)
S	Power spectra of the signal (W/Hz)
t	Time (s)
T	Temperature (K)
T_e	Electron temperature (J)
u	Particle velocity (m/s)
$\vec{u}$	Particle velocity vector (m/s)
U	Voltage (V)
x	Distance between two microphones (m)
Z	Ion charge number (-)
α	Phase shift between particle velocity and sound (rad)
β	Temperature coefficient (K^{-1})
γ	Coherence function (-)
ϵ_0	Permittivity of free space ($A^2.s^4/kg.m^3$)
η	Plasma resistivity (Ω.m)
∇	Nabla operator
Δf	Noise bandwidth (Hz)
θ	Angle between light beams (rad)
λ	Wavelength (m)
ν_{ei}	Electron ion collision frequency (Hz)
ρ	Density (kg/m^3)
σ	Plasma conductivity (S/m)
φ	Angle between magnetic flux and particle velocity (rad)
ψ	Deflection angle of magnetic field lines (rad)
ω_{ge}	Electron cyclotron frequency (Hz)

Contents

1 Introduction

The target of this work is to make proof of the new measurement concept by theoretical and numerical investigations. Those investigations include various topics from acoustic measurement methods to plasma physics and electronics. In this chapter, as a first insight into the topic the importance of intensity measurements in automotive applications will be introduced. In the problem definition, the concept of sound intensity is discussed with the relevance of sound pressure level and acoustic particle velocity to the sound intensity measurements. In this context, the importance of acoustic particle velocity measurements and its challenges are illustrated. Methods that are used in order to detect particle velocity are handled in two main groups, as automotive relevant and research relevant respectively. Principles of those methods are explained with their advantages and disadvantages.

1.1 Sound pressure and particle velocity

In experimental acoustics sound intensity measurements have great importance besides detection of sound pressure level. While the sound pressure level can provide information about how loud an environment is, sound intensity measurements can help to define the direction and magnitude of the emitted sound waves. This is a significant measure to detect the location of multiple sound sources and to calculate sound power. To visualize sound radiation from multiple sources a vehicle could be used as an example. When a vehicle is started, the sound is radiated from various components due to airborne and structure-borne disturbances. However, a sound pressure level gauge cannot detect sources of those disturbances one by one. To investigate the share of each component a sound intensity map is very useful. Sound intensity measurements allow generating sound intensity maps as seen in Figure 1-1. A sound intensity measurement unit combines signals of sound pressure and particle velocity related to their phase shift as in formula (1-1).

$$\vec{I} = \vec{u} \cdot p \cos(\alpha) \tag{1-1}$$

$\vec{I}$	*Sound intensity vector (W/m²)*
$\vec{u}$	*Particle velocity vector (m/s)*
p	*Sound pressure (Pa)*
α	*Phase shift between particle velocity and sound pressure (radians)*

The mechanism of sound propagation and relevance to sound intensity can be explained as follows. There is an instant rise of pressure when an air molecule is displaced from its original position. The pressure rise has two following effects. Firstly, to push the air molecule back to its initial position and secondly to conduct the disturbance to the next air molecule. This cycle of increases (compression) and decreases (rarefactions) in pressure propagates through the

medium as a sound wave. In this process, sound pressure illustrates the magnitude of pressure fluctuations and particle velocity is the oscillation rate of air molecules about a fixed position [1].

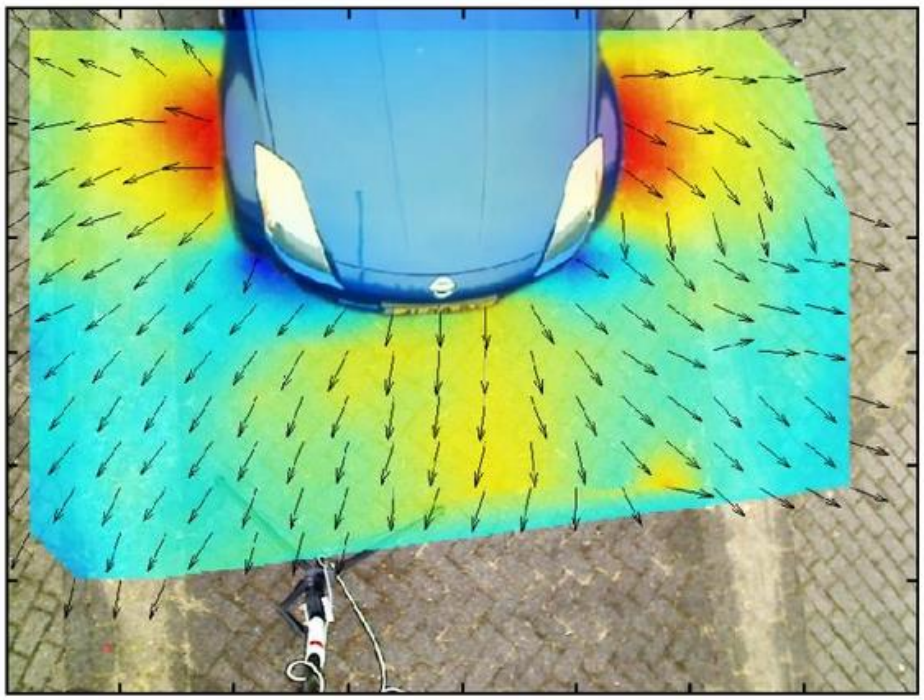

Figure 1-1 : Sound intensity vector field mapping of a car front [2]

Sound intensity is described as the product of particle velocity and sound pressure. Moreover, sound intensity can also be defined as sound power per unit area. Sound power is defined as below.

$$P = \iint_S \vec{I} \cdot d\vec{S} \tag{1-2}$$

P	*Sound power (W)*
$\vec{I}$	*Sound intensity vector (W/m²)*
$\vec{S}$	*Area vector (m²)*

As seen in formula (1-2) sound power is the rate of change in sound energy which is radiated from any vibrating substance. According to [1] the relation between sound power and sound pressure can be explained as follows. “A sound source radiates power, and this results in sound pressure. Sound power is the cause. Sound pressure is the effect. This could be explained with the following analogy. An electric heater radiates heat into a room and temperature is the effect. Temperature is also the physical quantity that makes us feel hot or cold. The temperature in the room is obviously dependent on the room itself, the insulation, and whether other sources of heat are present. But for the same electrical power input, the heater radiates the same power,

practically independent of the environment. The relationship between sound power and sound pressure is similar. What we hear is sound pressure, but it is caused by the sound power emitted from the source". As a result, sound intensity which is related to sound power stands as the correct measure to identify a sound field emanated from a sound source.

While measurements of sound pressure can be done with microphones, there are several ways to detect particle velocity. The reason why different techniques have been discovered is that measuring particle velocity comes with its difficulties. Each method has a specific area of application and corresponding requirements. According to the measurement setup, those methods can have advantages or disadvantages. One of the most significant challenges in those methods are calibration and sensitivity of sensing devices. Moreover, some methods are not useful for automotive applications due to high complexity and costs.

1.2 Acoustic particle velocity measurements – state of the art

In the old times sound power measurements required anechoic environments, but since the development of the dual mic probe sound intensity measurements can be carried out in many environments including around and inside cars, in engine test rooms. In this context, devices which are used for research such as Laser Doppler Anemometry and Particle Image Velocimetry are not very convenient. Moreover, the mobility of the measurement device is also a significant property. Those devices mentioned above requires a fix position and cannot be used as probes.

On the other hand, measurement techniques such as the two-microphone method and hot wire/film anemometry can be used as probes. This provides mobility required to locate the probe in or around the vehicle. In this chapter, both methods are discussed.

1.2.1 Practical industrial methods

As the mobility and size of the measuring probe is an important property, the following methods are explained in this chapter which are practically used in automotive. To detect particle velocity, two-microphone method, hot wire/film, or double hot wires can be used. Each method has advantages and disadvantages which are explained in this chapter.

1.2.1.1 Two-microphone method

By measuring particle velocity, one must consider the whole measurement chain including properties of the measurement medium. In case of acoustic particle velocity measurements mostly air is the medium through which sound waves propagates. In the air, sound pressure can be detected with a single microphone without problems. On the other hand, measuring particle velocity is not as simple. The particle velocity, however, can be related to the pressure gradient (the rate at which the instantaneous pressure changes with distance) with the linearized Euler equation [1]. This equation enables one to calculate particle velocity from the pressure gradient obtained from two closely located microphones as seen in Figure 1-2.

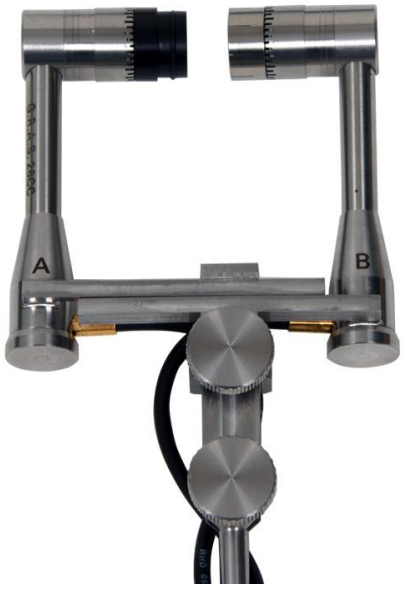

Figure 1-2: Sound intensity probe with two microphones [3]

To derive the Euler's equation similar approach to Newton's second law must be applied to a fluid. According to Newton's second law (1-3), if the mass and the force exerted are known, the acceleration can be calculated. By integrating acceleration over time, the velocity can be obtained (1-4).

$$F = m.a \tag{1-3}$$

$$u = \int \frac{F}{m} dt \tag{1-4}$$

F	*Force (N)*
m	*Mass of fluid element (kg)*
a	*Acceleration (kg/m³)*
u	*Particle velocity (m/s)*
t	*Time (s)*

In Euler's equation instead of exerting force, a pressure gradient accelerates a fluid with a certain density. Take a plane wave propagating in the *x*-direction, take a small cylindrical volume of length *dx* and constant cross-section surface area *S*. The mass of the enclosed fluid is m according to (1-5), and the force acting on the volume element is F according to (1-6). Therefore, substitution in (1-4) yields referring to [1].

$$m = \rho S dx \tag{1-5}$$

$$F = -Sp(x + dx) + Sp(x) \tag{1-6}$$

$$u = -\frac{1}{\rho}\int \frac{\partial p}{\partial x} dt \tag{1-7}$$

u	*Particle velocity (m/s)*
ρ	*Air Density (kg/m³)*
p	*Sound pressure (Pa)*
x	*Distance between two microphones (m)*

The pressure gradient in formula (1-7) is a function which describes the rate of change of pressure with respect to distance. The distance is determined by the spacing between the two microphones. As the pressure gradient is a continuous function a finite difference approximation must be made for the space derivative. This approximation gives rise to numerical errors. The finite difference errors, however, become very small when the microphone spacing is small compared with the governing wavelength, by using different spacers the error remains very small (< 1dB) in the full frequency range. The dual-microphone measurement is consequently very reliable and tailor-designed calibrators and methods like mike-switching allow for fine phase matching. The big problem of the methods are measurements in reactive sound fields and measurements very close to objects (reactive nearfield, interference of the probe with the sound field). The reactivity index of the field is, therefore, an important parameter.

1.2.1.2 Hot wire and hot film sensor

The relationship between electrical resistance and temperature can be used for various purposes in sensors. In an electric circuit resistance of a resistor element in formula (1-8) increases with rising temperature according to [4].

$$R = R_r(1 + \beta(T - T_r)) \tag{1-8}$$

R	*Resistance at operating temperature (Ω)*
R_r	*Resistance at reference temperature (Ω)*
β	*Temperature coefficient (1/K)*
T	*Operation temperature (K)*
T_r	*Reference temperature (K)*

This principle can be used to detect flow velocity by relating the temperature variance of the resistor to convective heat losses. For this purpose, a thin wire made of platinum, platinum-coated tungsten, or a platinum-iridium alloy can be used [4].

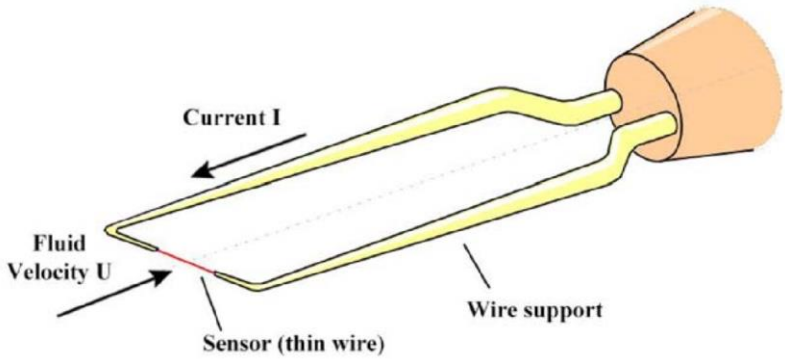

Figure 1-3: Hot wire sensor setup [5]

Operation of a hot wire sensor can be explained as follows. A current I, seen in Figure 1-3 is fed through the wire which leads to an increase in wire temperature. Once the wire with resistance R_w is heated enough for the application a flow whose particle velocity u is to be measured passes around the wire. Due to the flow, heat convection occurs around the wire which stops the increase of the wire temperature. When the temperature equilibrium is reached, the control resistance R_1 takes a higher value which results in a voltage difference E_B in measurement circuit with R_2, R_3 bridge resistances with current I as in Figure 1-4 below. This voltage difference E_B is amplified via an amplifier to a voltage E (bridge voltage out) can then be correlated with a flow velocity according to sensor calibration. However, with this method only a steady-state flow measurement is possible. As the absolute velocity is measured information about the direction of flow is not provided.

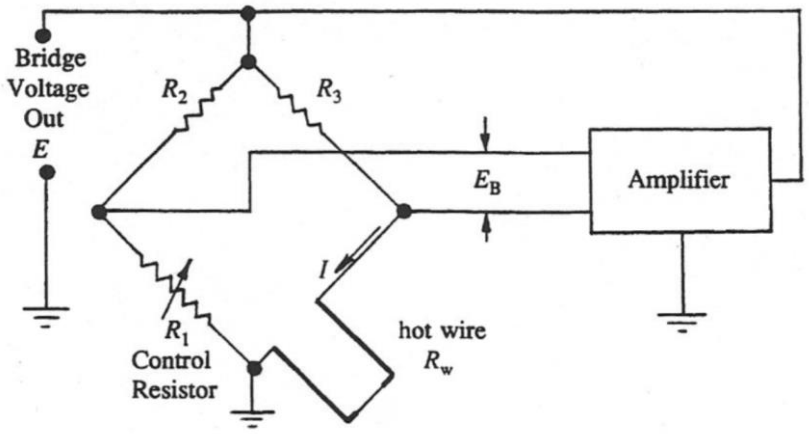

Figure 1-4: Hot wire sensor circuit [6]

To overcome difficulties due to sensitive construction of hot wire sensors, an alternative method was designed. The method uses a hot thin film instead of a wire with a similar working principle. As seen in Figure 1-5 when air flows over a thin film a temperature difference arises between two ends of the film. This temperature difference is compared with a temperature distribution curve can be seen in Figure 1-5. The deviation from the initial curve which was obtained in the absence of flow is related to air velocity. Thanks to higher durability and hot film compared to a thin wire, the hot film sensor can be used both in liquid and gas medium. The thin film is protected with an aluminium coating in case the sensor is in a gas medium, or quartz if the sensor is in a liquid to provide robustness to the sensor [4].

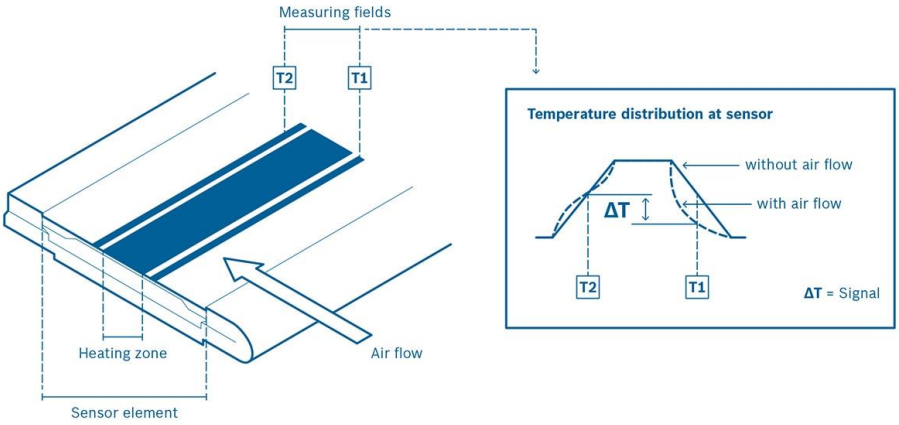

Figure 1-5: Hot film sensor [7]

Both hot wire and hot-film sensors have high response time which makes difficult to detect high sound frequencies. Those sensors are designed to measure a steady gas flow since the measuring mechanism requires a mass flow which causes convective heat transfer between the gas and hot surface. Hot wire sensor has also another disadvantage that only the absolute value of the flow velocity can be detected. The direction of the flow can't be distinguished.

1.2.1.3 Double hot wire sensor (Microflown)

The first development of double hot wire sensor has been done at University of Twente as part of PhD thesis of De Bree [8]. Double hot wire sensors are invented to overcome difficulties and disadvantages in hot wire sensors. In case of a single hot wire, the wire attains a temperature at equilibrium under steady flow conditions. However, the measurement can be done only of one-directional flows. When 2 wires are located closely, a slightly different principle is used. The wire in the upstream of flow is subjected to direct airflow while the wire in downstream is less effected from flow since it lays behind the first wire in upstream [8]. In this way, the direction of flow can be obtained.

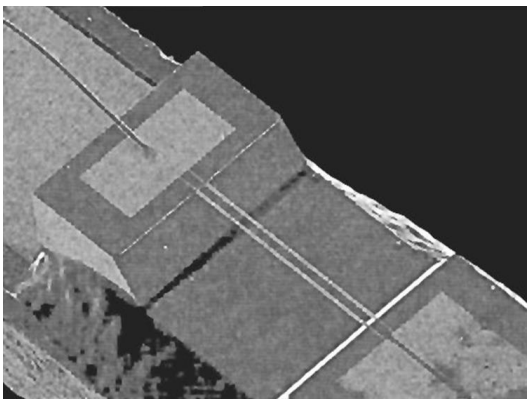

Figure 1-6: SEM photo of double hot wire sensor [8]

Seen in Figure 1-6 a very small gap of 40 μm separates two wires. To get enough temperature difference between wires the sensor is heated until the wires reach about 400-600K [9].

Although, its capability to detect flow velocities in two directions, as an anemometer based on effects of convective heat transfer, it has also limitations seen in Figure 1-7 with respect to the environment in which the sensor is operated [10].

Temperature range	-20 to 85 °C
Temperature Coefficient	0.006 dB/°C
Influence of Humidity (30 - 90%)	0.06 dB/%HR
Static Pressure Coefficient	< 0.5 dB/kPa
Maximum airflow	1.5 m/s

Figure 1-7: Environmental limitations for double hot wire operation [10]

Moreover, the double hot wire sensor is sensitive to superimposed constant airflow which makes calibration of those devices difficult. If the measurement has to be done where a secondary flow exists, for example a superimposed wind breeze (secondary flow apart from the flow to be measured), errors occur due to additional forced convection. In sound pressure level measurements this problem can be tackled by using wind balls. Wind balls can stop the superimposed flow component so that the measurement unit stays unaffected. However, this approach can not be used in the double wire method as the direction of flow is offset by wind ball. This offset gives rise to errors in the measurement.

1.2.2 Laboratory methods

To measure particle velocity in different applications, various measurement setups are designed. Those methods require the application of expensive and complex parts such as high-speed cameras and photodetectors. In this chapter, laser Doppler anemometry and particle image velocimetry are explained with their measurement principles. Moreover, the concept of magnetic flowmeters and corona discharge velocimeters are introduced. Those two methods illustrate a basis for the novel measurement method which is treated in chapter 2.

1.2.2.1 Laser Doppler Anemometry (LDA)

Laser Doppler Anemometry is an optical measurement method to detect flow velocity which provides determination of steady-state as well as transient flows with very high spatial accuracy [11]. Measurement principle in detail is explained in Figure 1-8 below. “Two laser beams crossed and focused, define a measuring volume in which an interference pattern, made of bright and dark fringes, appears. A seeding particle scatters light while crossing this volume. This light is detected by a photodetector and its intensity is modulated with a frequency, usually called Doppler frequency F_D”.

$$F_D = vD = v2sin(\theta/2)/\lambda \tag{1-9}$$

$$i = \frac{\lambda}{2sin(\theta/2)} = \frac{1}{D} \tag{1-10}$$

v is the component of the velocity $\vec{V}$ perpendicular to the fringes, λ the laser wavelength, i wavelength of reflected light and θ the angle between beams, and D as Doppler shift. In order to avoid ambiguity on velocity sign, the interference fringes are shifted with the help of a Bragg cell at $F_B = 40\ MHz$. Finally, the signal is downshifted thanks to a Quadrature Demodulation (QD) technique [12]. Thus, the estimation of F_D leads to particle velocity.

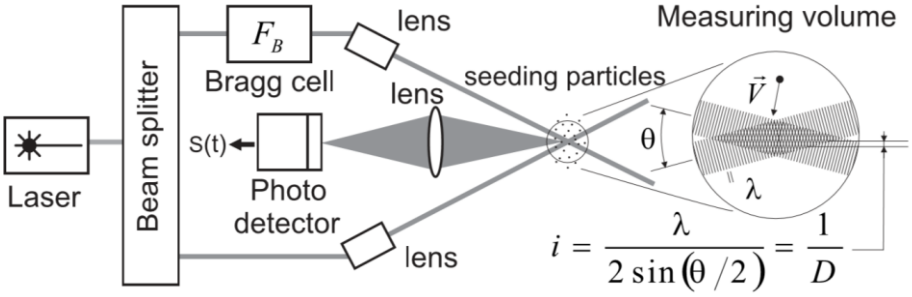

Figure 1-8: Setup Laser Doppler Anemometry [12]

Application of LDA could be very useful for sensing complex acoustic fields. However, LDA is not a common method in acoustics yet due to characteristics of acoustic signals having low magnitudes and high frequencies [13]. On the other hand, the high complexity of LDA does not allow practical usage for most of the applications in acoustics.

1.2.2.2 Particle Image Velocimetry (PIV)

Particle image velocimetry (PIV) is an optical method used for multidimensional flow visualization. Thanks to particle image velocimetry instantaneous measurement of a field of vectors can be illustrated non-intrusively. This method has a wide area of application from the motion of ocean waves to acoustic streaming [14].

In particle image velocimetry the fluid to be measured is filled with tracer particles which are small and light enough to follow the dynamics of the fluid flow (particles should be neutrally buoyant). The fluid is then illuminated in the target area with a laser sourced light-sheet reflected from a mirror seen in Figure 1-9. A camera captures each light pulse in separate image frames. By comparing those images at time t and t' each particle can be traced. Dislocation of tracer particles gives a vector which can be used to generate a vector map of the flow.

Although its capabilities of visualization of flow fields, particle image velocimetry setup is a complex system which makes the method inconvenient for many applications. Moreover, in terms of acoustic measurements illumination and recording synchronization can be challenging when a high sound intensity needs to be detected. “Increasing the sound intensity level in order to gain higher amplitudes of acoustic motions may cause two undesirable effects. First, this increments the acoustic velocity which demands higher temporal PIV sampling and, consequently, shrinks the PIV ranges. Secondly, increasing the amplitude in this way can create some unwanted non-linear events such as distortion or streaming” [15].

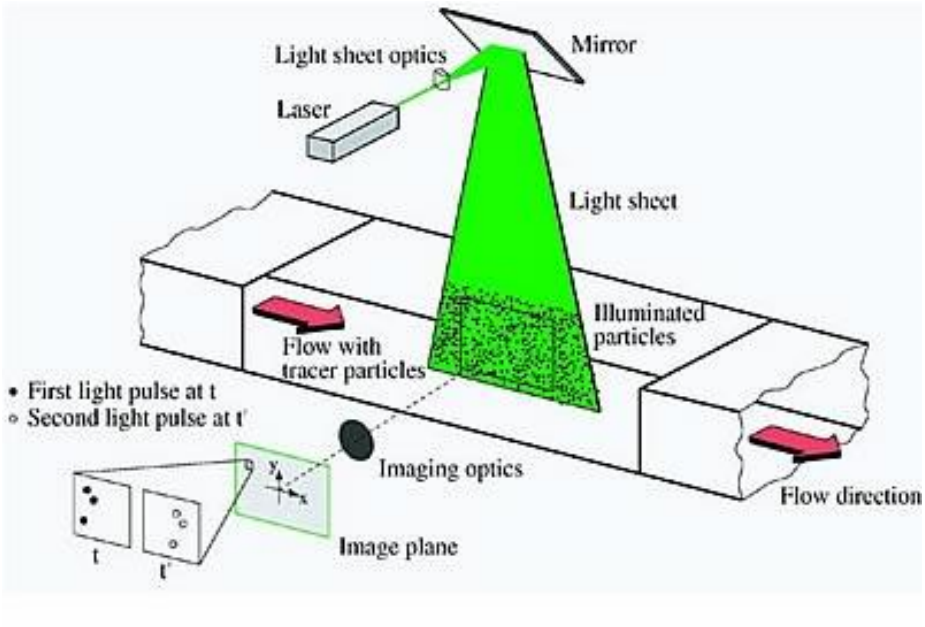

Figure 1-9: Typical PIV Setup [16]

1.2.2.3 Magnetic Flowmeter

Magnetic flowmeters are one of the most widely used devices used in piping systems for flow measurements. Thanks to its construction and measurement methodology, magnetic flowmeters are non-invasive devices which allow highly sensitive detection of flow velocity. Moreover, magnetic flowmeters can be also used in harsh environments including flow measurement of abrasive fluids. Magnetic flowmeters can also measure bidirectional flows and are insensitive to viscosity, density and flow disturbances [17].

Faraday's law of electromagnetic induction is the key principle applied to magnetic flowmeter operation. Faraday's law states that a voltage will be induced in a conductor loop moving through a magnetic field. The magnitude of the induced voltage is directly proportional to the velocity of the conductor, the width of the conductor, the strength of the magnetic field and the angle between velocity and magnetic field seen in formula (1-11). In most applications, the installation of the flowmeter is made in a way that flow velocity and magnetic field lines are perpendicular as seen in Figure 1-10 so that the last sine term equals to 1. According to this assumption, the formula for particle velocity derived from Faraday's Law is stated in formula (1-12)

$$U_E = B.u.L.\sin(\varphi) \tag{1-11}$$

$$u = \frac{U_E}{B \cdot L} \tag{1-12}$$

U_E	*Signal voltage (V)*
B	*Magnetic flux density (T)*
u	*Particle velocity (m/s)*
L	*Distance between electrodes (m)*
φ	*Angle between B and u (radians)*

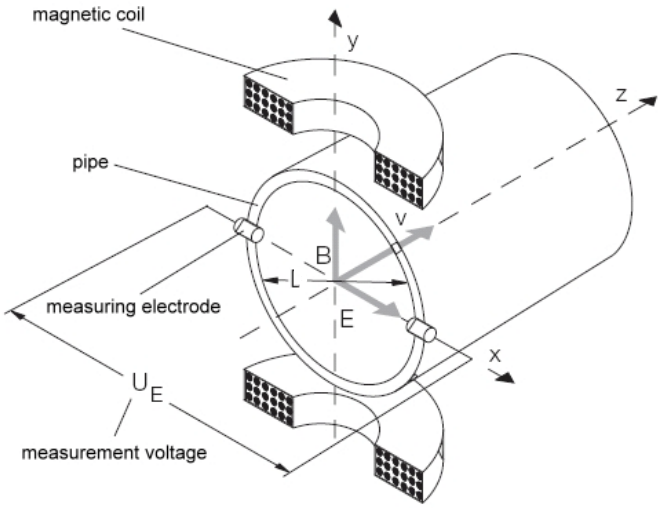

Figure 1-10: Magnetic flowmeter [18]

For the operation of a magnetic flowmeter following components must be in the measurements setup also seen in Figure 1-10. A flow tunnel, for example, a pipe in which a fluid can flow. The inner layer of the pipe must have an electrically insulating material to avoid noise generation due to fluid flow and to avoid short circuits in the measurement chain. Permanent or coil magnets to provide a magnetic field perpendicular to flow. Last but not least, two electrodes on each side of the pipe to detect induced voltage.

Besides significant advantages mentioned previously, magnetic flowmeters can also be disadvantageous for some applications. The limitations of electromagnetic flowmeters can be listed as [17]

1. The meters work only with conductive fluids. Air particle velocity cannot be measured.

2. Electrical installation care is essential.

3. The price of magnetic flowmeters ranges from moderate to expensive. Their corrosion resistance, abrasion resistance, and performance over wide turndown ratios can justify the cost. Ceramic and probe type units are less expensive.

4. To periodically check the zero on AC-type magnetic flowmeters, block valves are required on either side to bring the flow to zero and keep the meter full. Cycled DC-units do not have this requirement.

5. An important limitation in electromagnetic flowmeters may be the effect of magnetohydrodynamics, which is especially prominent in fluids with magnetic properties. Magnetohydrodynamics refers to the ability of magnetic field to modify the flow pattern. In some applications, the velocity perturbation due to the magnetohydrodynamic effect may be serious enough to influence the accuracy of operations.

Among the limitations above electrical conductivity is the decisive parameter for the operation of magnetic flowmeters. The unit of electrical conductivity is siemens per meter which is reverse of electrical resistivity. Requirements for minimum conductivity can differ depending on the application, however, it can be stated that 5 micro siemens per centimetre is minimum conductivity limit is for liquids. When conductivity is below this limit, the resistance of the electrode can generate an error in the velocity signal [19].

1.2.2.4 Corona Discharge Velocimeter (state of the art)

Corona is a type of gas discharge which occurs between two electrodes, one plane the other with curvature. The curvature generates a high potential gradient around the electrode for plasma generation. For corona generation arcing should not occur between electrodes. Instead of instantaneous arcing, electrons drift from curvature to planar electrode through the drift region "d" as seen in Figure 1-11. Thanks to non-arcing plasma generation a plasma plume can be obtained.

When a voltage of 3-12kV is applied between two electrodes, the gas is ionized, meaning that charged particles are created. The flow of these particles from one to another electrode leads to an electric current in the external electric circuit. "For a given range of high voltages V_{HV} above a threshold voltage V_s, the electric current I, which is over resistance R, consists in regular pulses (known as, "Trichel pulses"), with a repetition rate around a few hundred kHz (far higher than audio frequencies: 20 Hz - 20 kHz). As the voltage is increased, the pulses turn into a steady-state current regime (glow discharge) until a spark occurs. In the Trichel pulses regime, the frequency of the pulses depends on various factors such as the geometrical and electrical configurations of the electrodes but also on the surface properties" [20].

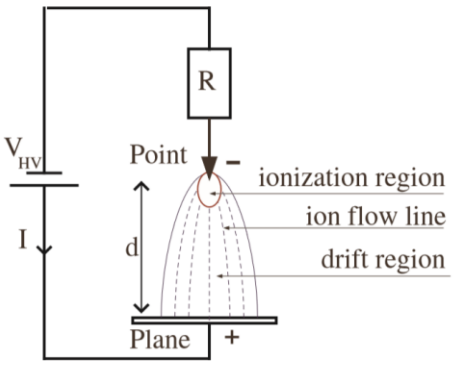

Figure 1-11: Corona Discharge Formation [20]

The measurement principle is based on the detection of the movements of ions influenced by the displacement of the air particles due to a sound wave. The generation of these ions is performed by a negative point-to-plane corona discharge. Negative corona discharge refers to that curvature electrode dominantly has negative ions compared to the planar electrode. When

there is no acoustic perturbation the current measured is the same on planar electrodes ($I_1 = I_2$) because of the straight path of electrons. When ionized gas is subjected to acoustic perturbation, the trajectory of ions is deflected as seen in Figure 1-12, which gives rise to less or more charges on measuring electrodes. The current difference between two planar electrodes is then a measure of acoustic perturbation and the acoustic particle velocity [20].

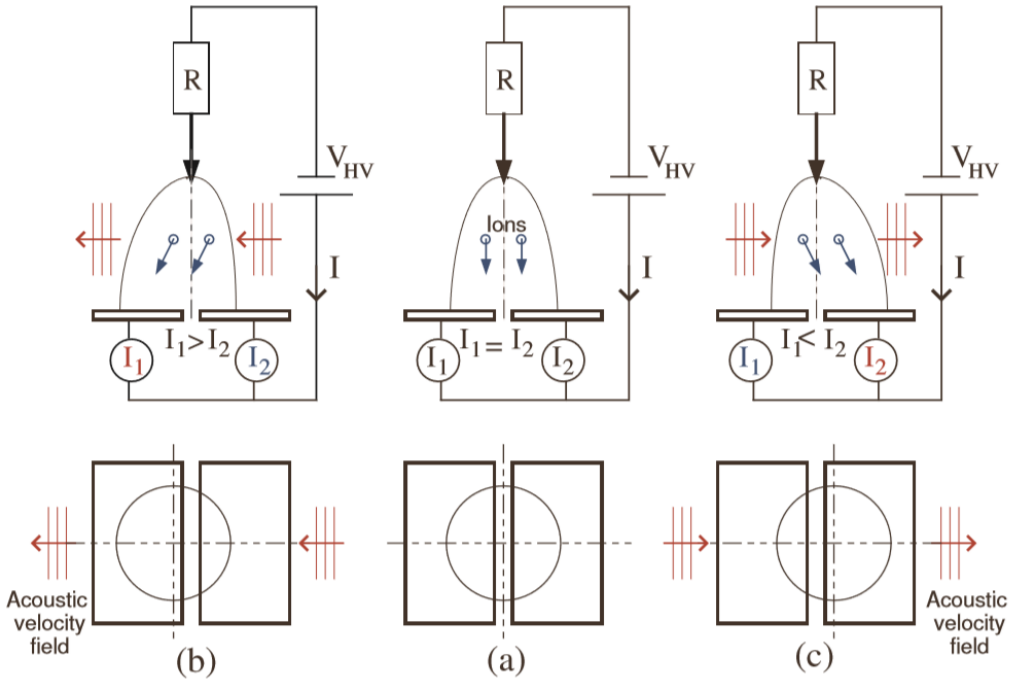

Figure 1-12: Measurement principle of corona discharge velocimeter [20]

1.3 Conclusions and work content description

According to comparisons and investigations have been made about methods to measure acoustic particle velocity each method has disadvantages such as high complexity, low mobility, and difficult calibration. A novel method which overcomes one or more of these disadvantages could be a breakthrough. In the following chapter, the new measurement concept is introduced. Afterwards, the theoretical background required to define parameters and limitations is presented. Moreover, the design of a measurement setup is proposed. Finally, the feasibility of the measurement method is discussed according to the proposed measurement setup.

2 The new measurement concept: Plasma particle velocity sensor (PPVS)

Researchers at the Virtual Vehicle Research GmbH in Graz had an initial idea to measure particle velocity with plasma application. The method first has appeared in a patent application [22] of the measurement concept. The target of this research is to investigate the feasibility of the above-mentioned novel method to measure particle velocity. This new method is based on the magneto-inductive principle like magnetic flowmeters. Magnetic flowmeters require a conductive liquid flow thus cannot be used to detect particle velocity in air. In this method, the air is ionized by plasma generation to provide the required conductive medium for a measurement based on the magneto-inductive principle. There are various ways to generate plasma, however, the plasma generated must be hanging in the air as free as possible distant from surrounding objects. The reason why is that acoustic waves must interact possibly with plasma to avoid sound wave reflections and scattering due to surrounding objects. Another aspect which must be taken into account is that the method is meant to be used in automotive applications. In this context, the measurement device must be the hand-held size and must allow safe operation. Thus, plasma sources like plasma torches that have operation temperatures between 2000-20.000 Celsius [21] are not suitable. Instead, commercially available cold plasma devices can be used to generate plasma which is at room temperature or a maximum of 50 degree Celsius. Plasma jets, dielectric barrier discharges, and piezoelectric direct discharges are the methods that are investigated for this application.

The size of the plasma generated has a crucial effect on the measurement. If the plasma length is bigger than the acoustic wavelength, a modal behaviour of the plasma can be expected [20]. In this case, the interaction of the magnetic field and plasma come into question which could lead to the speed of sound changes in certain conditions. This effect is investigated in chapter 3.11.2. Moreover, the acoustic field has effects on the magnetic field which could lead to a deviation of the axial magnetic field lines seen in the next page (y-axis in Figure 2-1). When the magnetic field lines are not perfectly perpendicular to the acoustic field, this effect must be taken into account while calculation of the induced voltage. An investigation has been done to this context in chapter 3.11.1.

The concept of the new measurement method is explained as follows. Assuming that a fluid which is not conductive, for example, air molecules, oscillating in x-direction as shown in Figure 2-1. A constant magnetic field in the y-direction is applied to the area of measurement which is between two measuring electrodes. If the fluid is locally (between electrodes) made conductive, this will give rise to an induced potential in z-direction which is proportional to instantaneous fluid velocity [22].

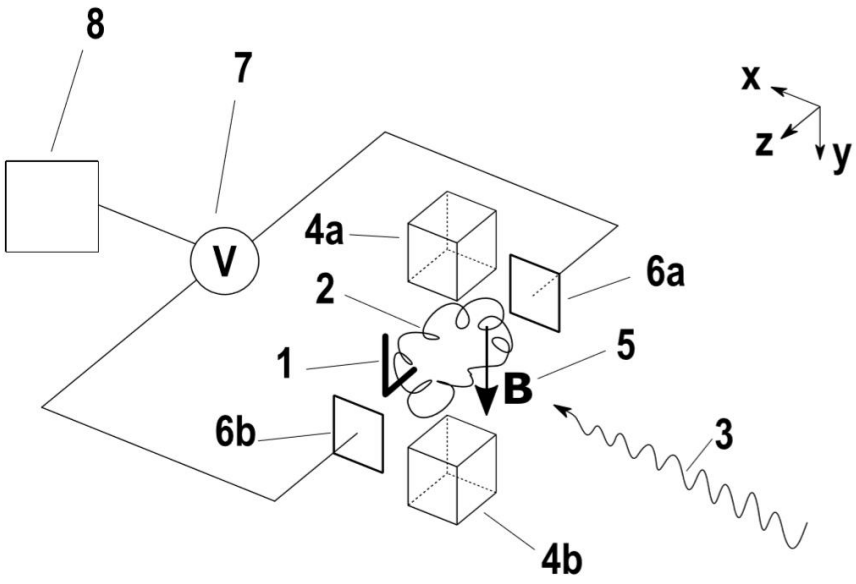

Figure 2-1: Concept of the novel measurement method [22]

The operation principle of the new method has the following steps [22]:

- In the first step, a plasma generator (1) creates a conductive medium, in other words, plasma (2)
- In the second step, a magnetic field B is created by means of coils (AC or DC) or by means of permanent magnets (4a) and (4b) providing an axial magnetic field on the entire measurement section.
- In the third step, the measurement section is exposed to a sound field (3) causing the oscillation of the plasma
- In the fourth step, the voltage induced due to the oscillations of the conductive plasma inside the magnetic field is determined by an arrangement of electrodes (6a) and (6b), and a voltage measurement unit (7). The polarity of the measurement signal indicates the orientation of the particle velocity vectors.
- In the fifth step, the sound velocity is compensated in a calculation unit (8) if required (i.e. if the size of the measurement volume is not much smaller than the acoustical wavelength).
- In the sixth step, the particle velocity is calculated based on the determined voltage according to Faraday's formula.
- In the seventh step, the calculated gas-particle velocity is provided as output value over time.

2.1 Forces exerted on charged particles

As mentioned in the previous chapter the measurement principle is based on Faraday's law of electromagnetism. To be more precise on applying Faraday's principle, forces exerted on charged particles in plasma are explained below. Ionized air by the plasma has a large number of free electrons and much heavier ions. When charged particles are exposed to electric and magnetic fields those charged particles are subjected to Lorentz force seen in formula (2-1). In this application the first term $q\vec{E}$ vanishes resulting in formula (2-2)

$$\overrightarrow{F_L} = q\vec{E} + q(\vec{u} \times \vec{B}) \tag{2-1}$$

$$\overrightarrow{F_L} = q(\vec{u} \times \vec{B}) \tag{2-2}$$

$\overrightarrow{F_L}$	*Lorentz Force (N)*
q	*Charge number (C)*
$\vec{E}$	*Electric field (V/m)*
$\vec{u}$	*Particle velocity vector (m/s)*
$\vec{B}$	*Magnetic flux density (T)*

The Lorentz force acts for positive and negative charges in opposite directions (see in Figure 2-2) which leads to separation of charges. Due to this charge separation, a difference in electric potential emerges which allows measurement of the induced voltage. This induced voltage is then calculated with Faraday's formula of electromagnetic induction (1-10) identically as in magnetic flowmeters.

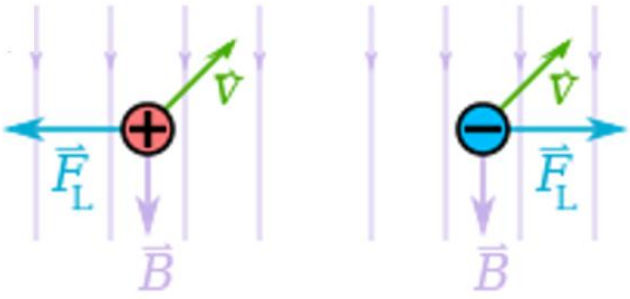

Figure 2-2: Lorentz force and charge separation [23]

2.2 Effects to be analysed for the feasibility of PPVS

To prove the feasibility of the PPVS several effects must be investigated. A detailed investigation follows in chapter 3. Those effects can be listed as follows.

- Effects of different plasma generation methods
- Order of magnitude of induced voltage and its effects
- Post-processing of induced voltage signal
- Importance of electrical conductivity and related limitations
- Magnetic field effects on plasma acoustics

Depending on the results of the evaluation in chapter 3 a test set up will be designed in chapter 4 focused on each component separately such as plasma generator, permanent magnet and voltage detection unit.

3 Analysis of interacting physical effects

In this chapter, the concept of plasma and related parameters are introduced. Initially, the concept of plasma and plasma generation methods relevant to this research are discussed. Subsequently, magnetic field strength exerted on plasma, and estimation of induced voltage due to a sound perturbation is calculated. According to the estimation of the induced voltage in plasma, which will be proven to be in the order of nanovolts, a suitable setup for the voltage measurement is proposed. Moreover, a possible post-processing method for the obtained voltage signal is presented.

In this new method, the electrical conductivity of generated plasma is crucial for the detection of the induced voltage. Thus, the concept of electrical conductivity is explained, and a simple model of electrical conductivity threshold for this measurement setup is generated. Afterwards, plasma parameters are introduced. According to parameter values, electrical conductivity is calculated to compare with the electrical conductivity threshold for the measurement. To conclude, plasma acoustics are treated to cover all relevant physical effects which could influence the feasibility of the method. Magnetic field effects on acoustic field are investigated and sound pressure level due to plasma generation are calculated.

3.1 Plasma generation

Plasma is the fourth state of matter which covers most of the universe. The word plasma refers to ionized gas to an extent that electrons are sufficiently energized to move freely away from the nucleus in a neutrally charged medium. Neutrally charged medium here means that same amount of positive and negative charges is coexisting in the plasma. Plasma can be found in many different forms. Examples would be ionosphere of the earth, fusion core plasma, corona and glow discharges seen in Figure 3-1. Those types of plasmas attain different properties depending on parameters illustrated in Figure 3-1 electron temperature T_e in Kelvin (y-axis) and electron density n in cm^{-3} (x-axis) enabling plasma usage in various fields of application. Laboratory plasmas i.e. glow discharges which are formed intentionally to ionize air or another application gas are the focal point of this thesis.

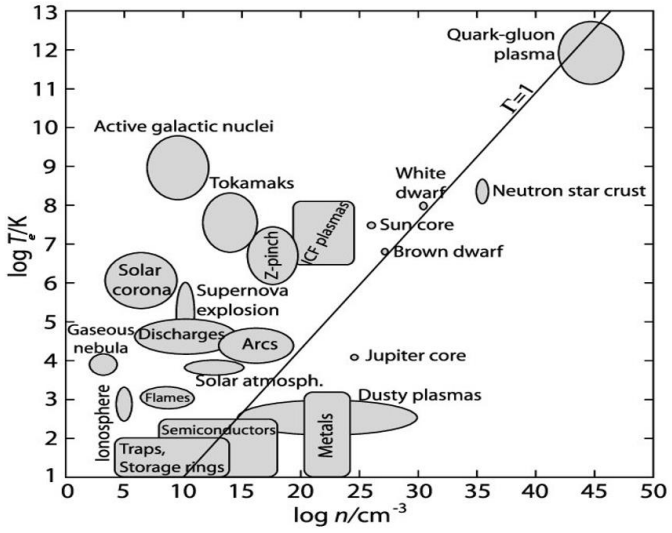

Figure 3-1: Plasma classification [24]

Plasma can be naturally found in the universe but can also be generated depending on application needs. Those generated plasmas can also be classified as laboratory plasmas since they are operated at atmospheric pressure conditions on earth in laboratories for research purposes. Laboratory plasmas are made of gas discharges by ionizing the medium gas or an external feed gas. As a result, the gas is partly ionized and contains the same amount of negative and positive charges.

There is a large number of techniques to generate gas discharges under atmospheric conditions. Werner von Siemens has first developed a dielectric barrier discharge reactor for ozone generation [25]. Afterwards, different designs and developments have been made in plasma generation for various purposes. Considering the new measurement method a few of those designs are investigated to determine the most convenient device for plasma generation. As the new measurement method requires a hand-held device, plasma generation has to comply with safety regulations to work in a closed environment. Moreover, the generated plasma must be cold (non-thermal plasma) and preferably with low noise radiation. Since an external magnetic field is going to be applied, a plasma with relatively low or no internal magnetic fields is preferable for testing purposes. Below possible plasma generation methods are discussed in order to select the most promising method for the acoustic particle velocity measurement.

3.1.1 Air pressure plasma jet (APPJ)

The air pressure plasma jet (APPJ) is one of the most common methods of generating cold plasma. The APPJ consists of two coaxial electrodes between which a feed gas (mixtures of helium, oxygen, and other gases) flows at rates up to 20 m/s [26]. The outer electrode is grounded while radio frequency (RF) typically around 13 MHz and power (50-100W) is applied to the central electrode that creates a discharge seen in Figure 3-2. The plasma produced exits the nozzle and arrives at the area that is to be treated. APPJ has been used in medical applications for the inactivation of several micro-organisms [27].

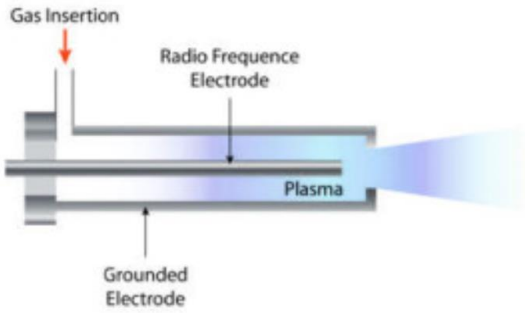

Figure 3-2 : Radio frequency plasma jet [26]

Apart from radiofrequency plasma jets which are driven by alternating current (AC), plasma jets can also be configured in a different way and can be driven with pulsed direct current (DC) with current pulses above 1MHz. According to [27] a plasma jet is designed which contains a dielectric cylindrical tube with 2.5 cm diameter in which two disk electrodes with the same diameter located seen in Figure 3-3. The gap between those electrodes can be set between 0,3 to 1 cm. The dielectric disk was coated with a thin copper ring. For plasma generation sub-microsecond high voltage pulses are applied between electrodes while a gas (typically N_2 or Ar) is injected through the holes of the electrodes.

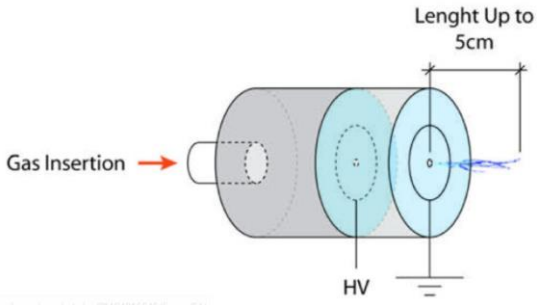

Figure 3-3: Pulsed current plasma jet [27]

The discharge is sprayed as a plasma plume from the cavity of the outer electrode outwards. Plasma generated is safe to touch thanks to its low temperature at 290K. The power supply used is a high voltage pulse generator which makes a special high voltage electronics element in the circuit necessary.

3.1.2 Dielectric barrier discharge (DBD)

Dielectric barrier discharge is historically the first laboratory plasma generation method discovered by Werner von Siemens [25]. The dielectric barrier discharge (DBD) consists of two metal electrodes that are covered with a dielectric material. Like plasma jets, one electrode carries high voltage and the other one is grounded. Plasma generation is achieved by the gas moving between electrodes. Different than in plasma jets, additionally a dielectric barrier is required to provide necessary charge accumulation for gas discharge.

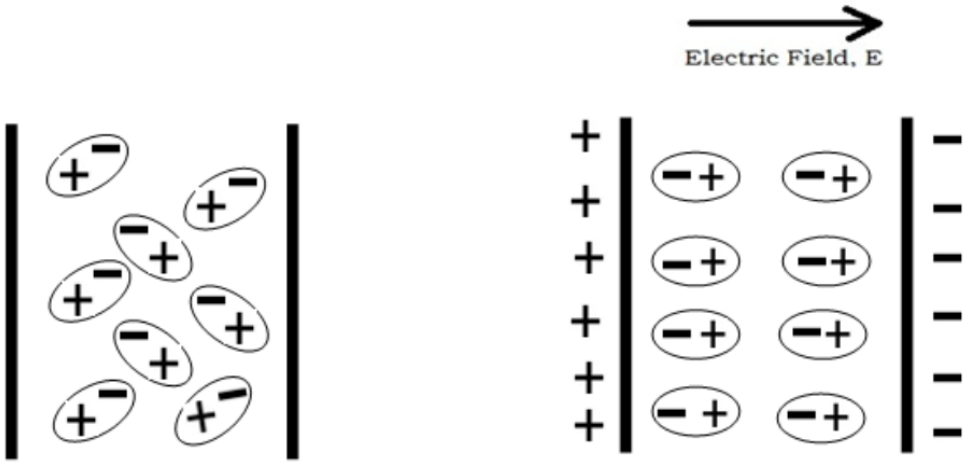

Figure 3-4: Concept of dielectrics [28]

To initiate the charge accumulation in the dielectric material, which is a good electrical insulator, a high voltage input is required. When alternative current (AC) at high voltage drive DBD with frequencies typically in the kHz range, a dielectric polarization process as seen in Figure 3-4 starts polarization of positive and negative charges which leads to the generation of electric field required for plasma generation in air. The power consumption is between 10W and 100W [29]. On the other hand, usage of a semiconductor layer of gallium arsenide (GaAs)

to replace the dielectric layer, allows DBDs to be driven by a DC voltage between 580V and 740V [30].

Due to the atmospheric pressure level, the plasma generation process requires high energy levels to sustain. Dielectric materials used in DBD are commonly glass, quartz, ceramics and polymers. “The gap distance between electrodes varies considerably, from less than 0.1 mm in plasma displays, several millimetres in ozone generators and up to several centimetres in CO_2 lasers” [29]. A variety of configurations of electrodes and dielectrics can be used while keeping the function and mechanism of the method same. Instead of flat electrodes, cylindrical electrodes can also be used to generate gas discharge. Different configurations of dielectric barrier discharge generation methods can be seen in Figure 3-5.

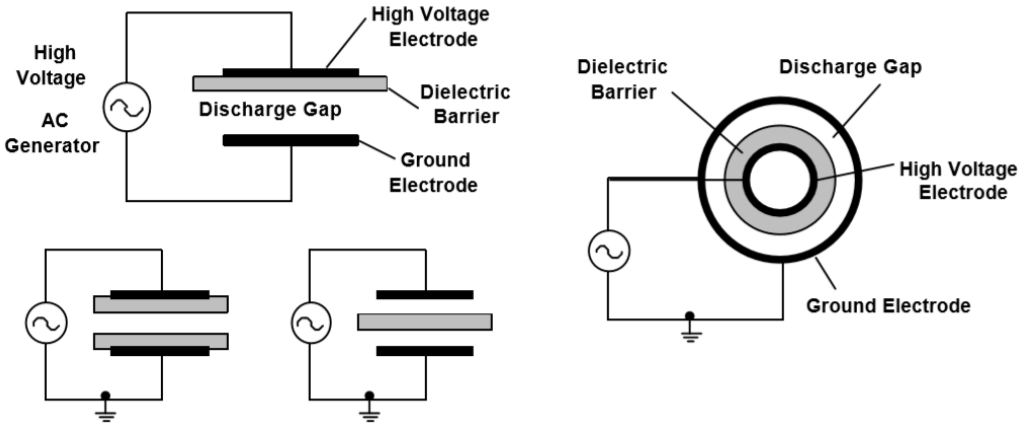

Figure 3-5 : Different configurations of dielectric barrier discharge [31]

Dielectric barrier discharge has initially been used to generate ozone. Moreover, it is used in industry for sterilization of materials and surfaces. It also illustrates a good basis as a methodology for this research, thanks to its plasma generation mechanism allowing a silent discharge. In a small volume confined, stable gas discharge helps to avoid sound generation in plasma.

3.1.3 Piezoelectric direct discharge (PDD)

DBD plasma generators can also be built in a more compact and economical way as piezoelectric direct discharge generator with similar operation manner. In piezoelectric direct discharge, high voltage is generated with a piezo-transformer principle in which secondary part (output section) of the piezo element and circuit works as a high voltage electrode seen in Figure 3-6. At certain frequencies, a mechanical resonance occurs which give rise to high voltages depending on material characteristics of the piezoelectric substance. Since transformer material has dielectric characteristics, the electric discharge generated has similar properties like dielectric barrier discharge which generates a cold non-equilibrium plasma. Non-equilibrium here refers to the condition that electron temperature is much higher than the temperature of ions and neutrals. As electrons and other species have different temperatures a thermal equilibrium does not exist. An advantage of this method is that a higher plasma generation efficiency is obtained with no external high voltage power supply.

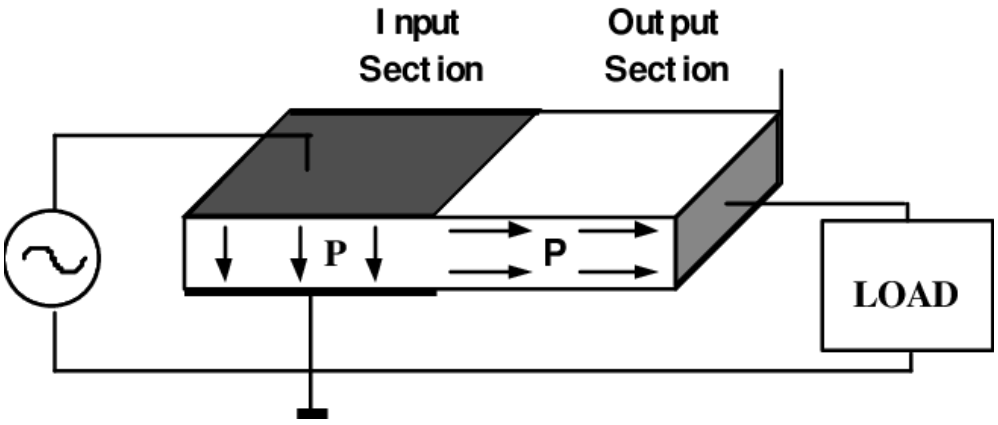

Figure 3-6: Basic structure of the Rosen type piezoelectric transformer [32]

The phenomena of piezoelectric effect on PDD works as follows. Initially, the microcrystals in piezo material are randomly oriented. To activate the material and start dielectric polarization of microcrystals a strong electric field must be applied. Once microcrystals align to the electric field as seen in Figure 3-7, a change in dimensions of the ceramic body occurs, too [33]. This effect allows a plasma generation with a low input voltage of 12V to 24V different and more efficient than all other plasma generation methods requiring only 10W of transferred power [34].

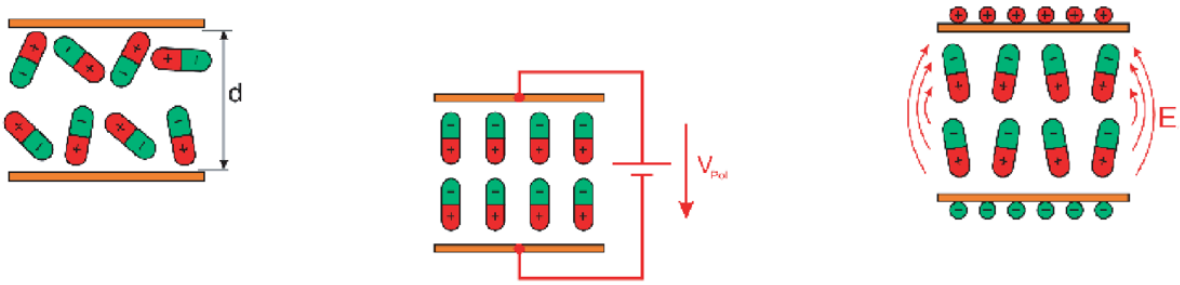

Figure 3-7 : Polarization in a piezoelectric direct discharge [32]

3.1.4 Comparison of plasma generation methods

Like introduced previously, there are 3 possible ways to generate cold plasma. Air pressure plasma jets (APPJ) generate a stable plasma plume under certain conditions. However, the complexity of these devices and high voltage electronic circuit make APPJ disadvantageous. Secondly, dielectric barrier discharge (DBD) generators are considered. As a plasma generation mechanism, dielectric discharge provides higher efficiency of plasma generation. Moreover, a silent stable discharge. However, this discharge is not compatible to be extended with airflow to a broader extent of few centimetres. Consequently, the piezoelectric direct discharge (PDD) method is investigated. In this method, the plasma generation mechanism is similar to DBDs. On the other hand, PDD does not require high input voltages like DBDs. This property makes PDD a more efficient plasma generator with a safer operation for a hand-held particle velocity measurement device.

3.2 Calculation of magnetic flux on plasma

Strength and direction of the magnetic field for this application has a significant effect on the induced voltage. For the sake of simplicity ring, permanent magnets are used for feasibility investigations. The axial magnetic field could also be generated with coil magnets, but the application of coil magnets would increase the complexity of the measurement setup.

Permanent ring magnets generate a constant axial magnetic field which must be perpendicular to particle velocity and voltage as it is necessary to apply Faraday's law of induction for the measurement. As the induced voltage linearly increases with an increasing magnetic field, a strong and compact ring magnet must be chosen for the measurement.

Figure 3-8: 4 permanent ring magnets stacked each other [35]

A typical ring magnet (with dimensions 40 mm outer diameter, 25 mm inner diameter, 5mm thickness) above in Figure 3-8 has a remanence field B_r of 1,29-1,30 T. However, for our purpose magnetic flux density on a certain distance of z seen in Figure 3-9 must be known. This distance z = 35, 40, 45, 50 mm is assumed to be axially from centre of each ring magnet's north pole face to the centre of the plasma plume. To calculate the exact magnetic flux density of each magnet on the plasma, the formula (3-1) is applied according to [36].

$$B = \frac{B_r}{2}\left[\frac{D+z}{\sqrt{R_a^2+(D+z)^2}} - \frac{z}{\sqrt{R_a^2+z^2}} - \frac{D+z}{\sqrt{R_i^2+(D+z)^2}} + \frac{z}{\sqrt{R_i^2+z^2}}\right] \quad (3\text{-}1)$$

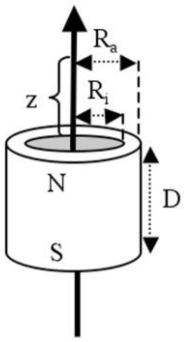

B: Magnetic flux density (T)

B_r: Remanence field (T)

z: distance from a pole face on the symmetry axis (mm)

D: Thickness of the ring (mm)

R_a: Outside radius of the ring (mm)

R_i: Inner radius of the ring (mm)

Figure 3-9: Dimensioning of ring magnet [36]

According to the specification of ring magnet and the formula above a magnetic flux density of B = 32,1 mT is obtained in the centre of plasma plume if 4 magnets will be stacked each other. The reason why z = 35 mm is selected as distance can be seen in Figure 3-10 below. A smaller distance than 35 mm to plasma would not be feasible because most PDD plasma generators have a piezoelectric element up to 35 mm which should not have any mechanical contact during operation due to vibrations. Moreover, when the distance is more than 35 mm, a natural decrease in magnetic flux density of the ring magnet is observed (see figure below). Therefore, the closest magnet to the plasma is placed at 35 mm and other 3 magnets are stacked to each other as seen in Figure 3-8.

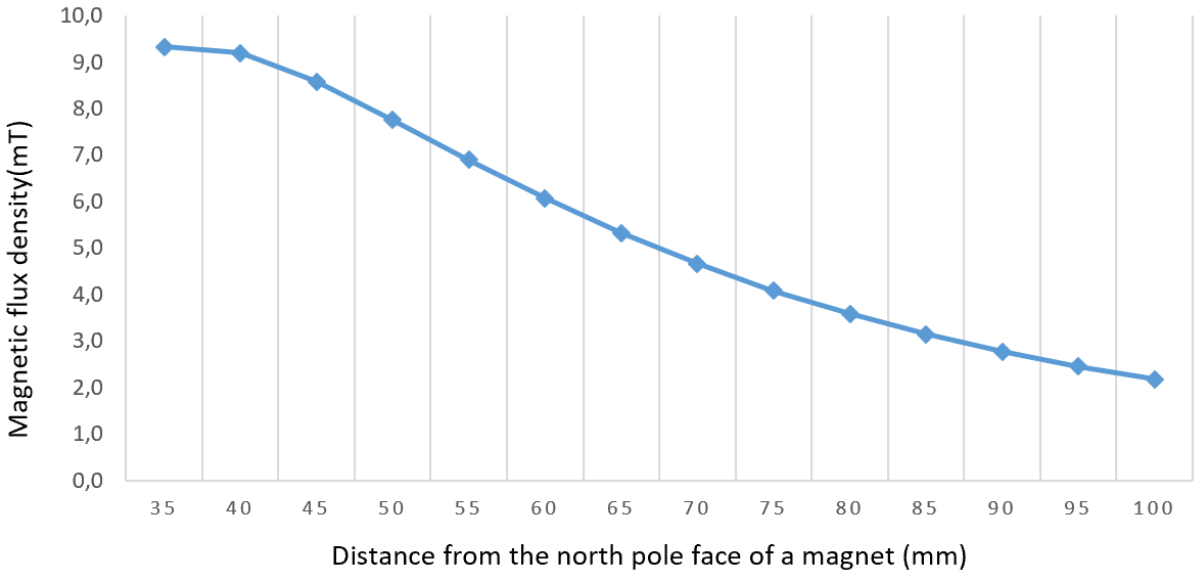

Figure 3-10: Magnetic flux density variation with distance z

For estimation of induced voltage and plasma parameters, a distance of z = 35 mm and cumulative magnetic flux density B = 32,1 mT of 4 stacked magnets are used in investigations. In chapter 4, the measurement setup will be more detailed presented considering all parts in the setup according to the output of theoretical investigations.

3.3 Estimation of the induced voltage

To make an estimation of induced voltage the following example is used. Initially, a sound source delivers L_p = 80 dB sound on plasma plume under standard conditions. According to formula (3-2), 80 dB corresponds to:

$$p = 10^{L_p/20} p_0 = \ 0{,}2\ Pa \tag{3-2}$$

If the air density ρ = 1,225 kg/m^3 and speed of sound c = 343 m/s assumed to be constant in air, and for the sake of simplicity assuming a plane propagating wave the particle velocity is determined according to formula (3-3)

$$u = \frac{p}{\rho c} = \ 4{,}76 \text{ x } 10^{-4}\ m/s \tag{3-3}$$

With a magnetic field of B = 32,1 mT and electrode spacing of L = 0,02 m the estimated induced voltage results as in (3-4)

$$U_E = B.u.L.\sin(\varphi) \ = \ 305{,}3\ nV \tag{3-4}$$

As the expected voltage is in order of nanovolts, voltage measurement and data acquisition of the induced voltage signal illustrate a great challenge in this research. In the following chapters, these two aspects are treated.

3.4 Measurement of the induced voltage

Detection of potential differences in nanovolt order of magnitudes is a challenging task. The signal detected by the electrodes is very weak and may be buried in the noise. To allow measurement with desired sensitivity (in order of nanovolts) a signal amplifier must be used. There are two types of signal amplifiers available, operational and instrumentation amplifiers. Operational amplifiers known as op-amps have the task to amplify voltage signals with electronic components like resistors and capacitors between in/out terminals seen in Figure 3-11 [37]

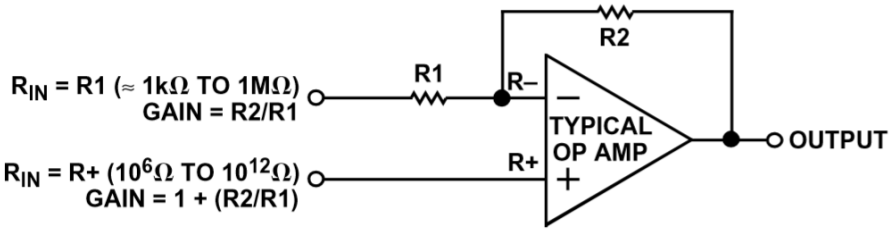

Figure 3-11 : Operational amplifier circuit [38]

However, op-amps lack accuracy in measuring low voltages due to their characteristics. The input resistance of the amplifier circuit here is a significant measure, typically between 10^9 to 10^{12} Ohms. "The measuring instrument input impedance controls the energy that is drawn from the source, or measuring system, by a measuring instrument. The power loss through the measuring instrument is estimated by $P = E^2/Z$ where Z is the input impedance of the measuring instrument, and E is the source voltage potential being measured. Thus, to minimize the power loss, the input impedance should be large" [4, p.39]. If a standard op-amp circuit were used for measuring low voltages in this research, the amplification effect would result in a gain in signal voltage and any direct current, noise or other common-mode voltages. Consequently, the signal would stay blurred under the noise, and the direct current offset [38]. Due to this property, even the best op-amps are far less effective in extracting weak signals which are important for our measurement. However, instrumentation amplifiers(in-amp) can tackle those problems mentioned. "An instrumentation amplifier is a device that amplifies the difference between two input signal voltages while rejecting any signals that are common to both inputs" [38]. Therefore in-amps are suitable for detection of small voltage differences.

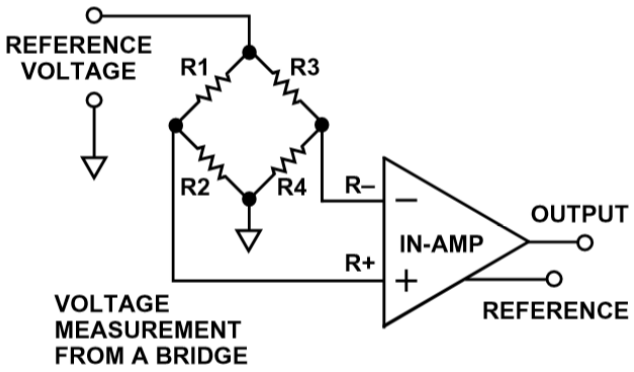

Figure 3-12 : Instrumentation amplifier circuit [38]

One of the most important functions which an instrumentation amplifier provides is the common-mode rejection. This function cancels out common signals while amplifying differential signals such as the potential difference between two inputs. Common mode rejection is formulated according to [38] in formula (3-5)

$$CMMR = A_D \left(\frac{V_{CM}}{V_{OUT}}\right) \tag{3-5}$$

$CMMR$	*Common mode rejection (-)*
A_D	*Differential gain of the amplifier (-)*
V_{CM}	*Common mode voltage at amplifier inputs (V)*
V_{OUT}	*The voltage at amplifier output when common-mode input signal applied (V)*

3.5 Post-processing of the signal

Another method in order to average the voltage signal out of the noise is coherence technique. Coherence in Latin means natural or logical connection or consistency. Coherence can be used to evaluate the similarity of signals and to find common frequencies [39]. Coherence function $\gamma_{xy}(\omega)$ is formulated according to [40] in formula (3-6)

$$\gamma_{xy}(\omega) = \frac{S_{xy}(\omega)}{\sqrt{S_{xx}(\omega) \cdot S_{yy}(\omega)}} \tag{3-6}$$

where S_{xx} and S_{yy} are power spectra of signals *x* and *y*. S_{xy} is cross-power spectrum for these signals and ω is frequency. Since a measurement over an infinite period of time is impossible a coherence estimation is performed with the usage of Fourier transformations of partially overlapping time blocks.

$$\gamma_{xy}(\omega) = \frac{\langle X^* Y \rangle}{\sqrt{\langle XX^* \rangle \cdot \langle YY^* \rangle}} \tag{3-7}$$

X and *Y* are the representation of *x* and *y* signals in the frequency domain seen in formula (3-7). The slanted brackets illustrate taking the average over time and/or frequency according to [41], [42]. Taking time average of the signal helps reducing noise in the signal by cancelling out noise elements in an imaginary plane. If enough number of the averaging procedure is done the cancellation of noise can be achieved as the signal converges to its noise values. In this application the measured variables are input voltage of loudspeaker V_{in} and the induced voltage in plasma V_p due to acoustic perturbance can be seen in Figure 3-17. The coherence function is written as follows.

$$\gamma_{V_p V_{in}}(\omega) = \frac{\langle {V_p}^* V_{in} \rangle}{\sqrt{\langle V_p {V_p}^* \rangle \cdot \langle V_{in} {V_{in}}^* \rangle}} \tag{3-8}$$

If the value of coherence function converges to one, this means that the difference between two voltage signals is negligible which is desired. In case the value of coherence converges to zero this depicts a situation that there is a significant amount of noise in the signal. The noise can then be filtered by the usage of specifically designed filters according to characteristics of noise such as voltage level and frequency bandwidth.

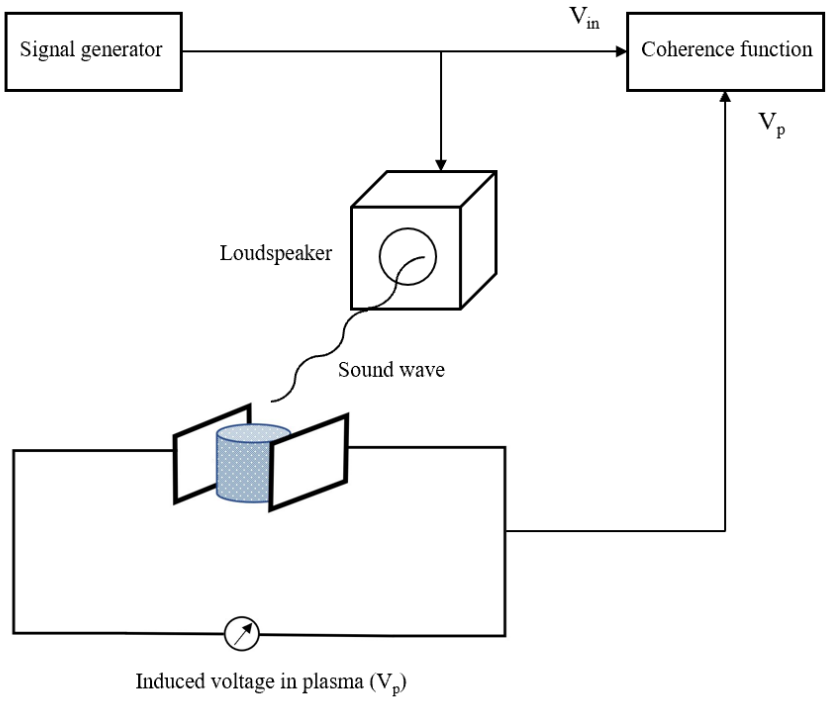

Figure 3-13: Data acquisition with coherence function

3.6 Importance of electrical conductivity on the measurement

In acoustic particle velocity measurements, the sensitivity of the measurement has great importance. In our case, measuring induced voltage depicts a challenge due to the fact that the magnitude of nanovolts is expected to be measured. For a reliable measurement, the conductivity of plasma must be at a certain level. "Conductivity is a measure of how an easily electric current can flow through a given material or medium" [43]. Conductivity is defined according to Ohm's law as below

$$\vec{J} = \sigma \vec{E} \tag{3-9}$$

$\vec{J}$	*Current density (A/m^2)*
σ	*Conductivity ($\Omega^{-1}m^{-1}$)*
$\vec{E}$	*Electric field (V/m)*

To measure a potential difference, a current flow through plasma plume is needed. According to the formula above (3-9), higher conductivity will result in higher current density for the constant electric field. Higher current density means more current will flow through plasma allowing more sensitive measurement.

Physics of plasma conductivity is slightly different compared to the conductivity of metals and electrolytes. In plasma, there are ions and negatively charged free electrons. Electrons contain

negligible mass compared to ions. Therefore, in the conductivity model of plasma ions are considered to be fixed while electrons are freely moving and colliding with heavier ions. According to this assumption mobility of electrons and electron density become a crucial measure for plasma conductivity.

3.7 Model of conductivity limitation for the measurement

For modelling the limitation of the conductivity, the closed-loop rule of Kirchhoff is used in formula (3-10). Assuming a current flows through the plasma so in the loop seen in Figure 3-18 we can derive the equation below.

$$U = I\left(R_p + R_V\right) = IR_p + IR_V \tag{3-10}$$

U	*Induced voltage (V)*
I	*Loop current (A)*
R_p	*Plasma resistance (Ω)*
R_V	*Voltmeter internal resistance (Ω)*

According to the equation above one can realize that measured voltage IR_v depends on the resistance of plasma plume and internal resistance of voltmeter.

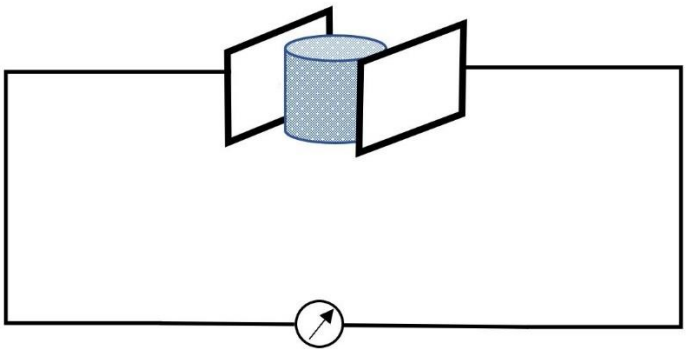

Figure 3-14 : Circuit for voltage measurement

Plasma resistance is the ratio of the length of the plasma plume L_p to conductivity σ in (3-11)

$$R_p = \frac{L_p}{\sigma} \tag{3-11}$$

For the measurement the plasma resistance R_p should be much smaller than the internal resistance of the voltmeter R_V ($R_V \gg R_p$). Conductivity limit is then defined as in the next page.

$$\sigma >> \frac{L_p}{R_V} = \frac{0{,}02\ m}{1\ G\Omega} = 2\ x\ 10^{-11}\ S\ /\ m \qquad (3\text{-}12)$$

To be able to measure a potential difference in plasma between electrodes we have to exceed well above the conductivity limit of $2\ x\ 10^{-11}\ S\ /\ m$ if distance between electrodes set L_ρ = 0,02m and internal resistance of R_V = 1 GΩ [38] according to formula (3-12)

3.8 Plasma parameters

In order to estimate the plasma conductivity, which is crucial for the feasibility of the method several plasma parameters must be known. In this research, a piezoelectric direct discharge is used to generate plasma. Thus, the values of parameters are only valid for this specific application.

3.8.1 Plasma frequency

Plasma is a dynamic state of matter including oscillations. When electrons are enough energized to move freely, they are displaced from initial positions which lead to the generation of electric fields in a direction to retain neutrality of plasma by towing electrons back to their initial positions.

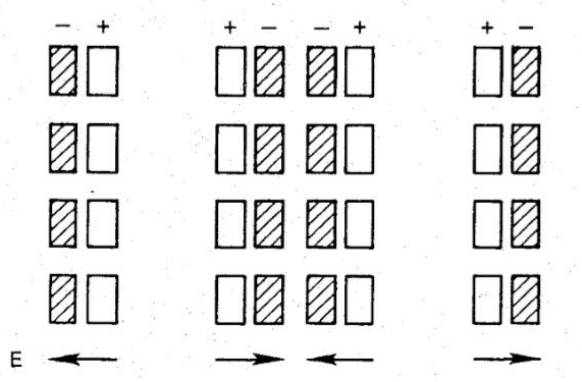

Figure 3-15: Oscillation of charges in plasma [44]

Due to their inertia, an overshoot will occur in an electron path and they will oscillate around their equilibrium positions seen in figure 3-19 with a certain frequency named plasma frequency. Much heavier ions cannot react with oscillating electron field and thus can be considered as fixed due to very fast oscillation of electrons [44]. The plasma frequency is defined with the formula below.

$$\omega_{pe} = \left(\frac{n_e e^2}{\epsilon_0 m}\right)^{1/2} \tag{3-13}$$

ω_{pe}	*Plasma frequency (Hz)*
n_e	*Electron density (1/m³)*
e	*Electron charge (C)*
ϵ_0	*Permittivity of free space (F/m)*
m	*Electron mass (kg)*

In the equation (3-13) electron density is the only variable considering the fact that electron charge e = 1,6 x 10^{-19}, the permittivity of free space ϵ_0 = 8,85 x 10^{-12} and electron mass m = 9,11 x 10^{-31} are constant in this application. However, the electron density is a very significant parameter in terms of mobility of electrons since electrons are the charge carriers which affect not only plasma frequency but also electrical conductivity. With constants above and electron density of n_e = 1 x 10^{-16} /m^3 for cold plasma generated with a PDD device according to [45] a plasma frequency of ω_{pe} = 20 GHz is obtained.

3.8.2 Electron cyclotron frequency (gyrofrequency)

For a measurement based on Faraday's law of electromagnetic induction, the plasma plume must be exposed to a magnetic field. When electrons move exposed to a magnetic field, their route is deflected by the electromagnetic force. In the case of no electric field, the path of electrons is illustrated as below in Figure 3-20.

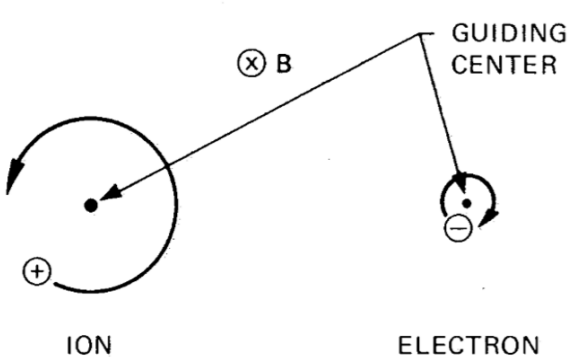

Figure 3-16: Gyration motion in the absence of an electric field [44]

Charged particles follow a helical path(gyration) along the magnetic field vector. Gyration direction is determined in a manner that a magnetic field generated by the charged particle is opposite to the externally imposed field. Thus, charged particles in plasma have a reducing effect for magnetic field making plasma diamagnetic [44].

When there is an electric field coexisting with the magnetic field the route of electrons and ions are deflected proportionally with a drift velocity of guiding centre v_{gc}. The motion is now a sum of gyration and drift of guiding centre with drift velocity seen in Figure 3-21. Electron cyclotron frequency is defined according to the formula below.

$$\omega_{ge} = \frac{eB}{m} \tag{3-14}$$

ω_{ge}	*Cyclotron frequency (Hz)*
e	*Electron charge (C)*
B	*Magnetic field strength (T)*
m	*Electron mass (kg)*

As the electron charge and electron mass depict constant parameters, decisive variable here is the magnetic field strength B = 3,21 x 10^{-2} T. This leads to a cyclotron frequency of ω_{ge} = 5,64 x 10^{9} Hz = 5,64 GHz according to formula (3-14).

3.8.3 Electron ion collision frequency

Electron ion collision frequency is the most significant parameter of plasma in this research as our focus is the conductivity of the plasma which is strongly dependent on electron mobility. Collisions in plasmas are not like the collision of solid objects in space. Electrons change their path due to Coulomb force in the proximity of ions and this is called an electron-ion collision. Coulomb force is defined as in formula (3-15)

$$F_c = -\frac{e^2}{4\pi\epsilon_0 r^2} \tag{3-15}$$

F_c	*Coulomb force (N)*
e	*Electron charge (C)*
ϵ_0	*Permittivity of free space (F/m)*
r	*Distance between charges (m)*

In the absence of Coulomb forces, an electron with momentum mv would follow a straight path with the closest approach distance of r_O called also "impact parameter". In the presence of Coulomb force, the electron will be deflected with a certain angle x from its straight path which is proportional to r_O [44]. This deflection in electron orbit restricts electron mobility which has a reducing effect on conductivity. Therefore, one can conclude that a higher rate of electron-ion collisions results in lower conductivity.

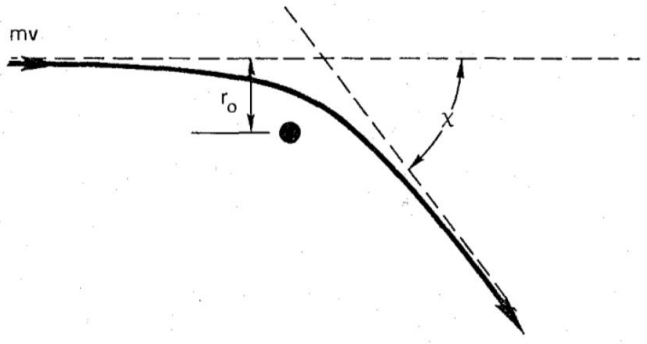

Figure 3-17: Orbit of electron colliding with ion [44]

Before deployment of electron-ion collision frequency calculation, one must first define the ionization level of the plasma. Plasmas can be classified into two groups in terms of the degree of ionization as fully ionized and weakly ionized plasmas.

For fully ionized plasmas a formula for electron-ion collisions can be derived from Spitzer's formula of conductivity. There are several formulations valid for different assumptions in literature. Assuming that in a fully ionized plasma ion and electron densities are the same to

comply with plasma neutrality, the definition of electron-ion frequency can be formulated in the next page referring to [46]. Before going into details of the formula (3-16) concept of electron temperature must be mentioned. In a cold partly ionized plasma the charged and neutral particles are not in thermal equilibrium. This means that while plasma as a gas volume having 50 degrees Celsius, the free electrons in plasma can attain high Temperatures typically around 60000 degrees Celsius. As the electrons have a negligible mass compared to neutral particles, the energy of electrons can be expressed either in energy units (Joules) or temperature units (degree Celsius or Kelvin).Therefore, electron temperature is defined and used in energy units (J) for convenience in plasma physics thanks to the proportionality between the electron temperature and the electron energy which is expressed with the Boltzmann constant k_B (J/K).

$$\nu_{ei} = \frac{2^{1/2} n_i Z^2 e^4 \ln \Lambda}{12\pi^{3/2} \epsilon_0^2 m^{1/2} {T_e}^{3/2}} \tag{3-16}$$

ν_{ei}	*Electron ion collision frequency (Hz)*
n_i	*Ion density (1/m³)*
Z	*Ion charge number (-)*
e	*Electron charge (C)*
$\ln \Lambda$	*Coulomb logarithm*
m	*Electron mass (kg)*
ϵ_0	*Permittivity of free space (F/m)*
T_e	*Electron temperature (J)*

For the formula above assuming that ion density $n_i = n_e$= 1 x 10^{16} m^{-3}, charge number of ions Z = 1 assuming that ions in the plasma are singly charged (O^{++} and such multiply charged ions are not existing), $\ln \Lambda$ = 10 as it is a cold laboratory plasma referring [44] and electron temperature T_e = 4,81 x 10^{-19} Joules according to [43] which results in an electron-ion collision frequency of ν_{ei} = 5,6 x 10^4 Hz indicating a highly conductive plasma property according to formula (3-16).

For weakly ionized plasmas contribution of ions in collisions can be ignored because the low ionization rate allows a high number of neutral atoms to exist in plasma plume. Instead, atom density has here a more significant role. In this case atom density n_a has a much bigger value than electron density n_e. The formula for electron-ion collision frequency is as follows according to [47].

$$\nu_{ei} = n_a q (T_e/m)^{1/2} \tag{3-17}$$

ν_{ei}	*Electron ion collision frequency (Hz)*
n_a	*Atom density (1/m³)*
q	*Average transport cross-section of electrons (m²)*
T_e	*Electron temperature (J)*
m	*Electron mass (kg)*

According to formula (3-17) atom density n_a = 1 x10^{21} referring to [48], average transport cross-section of electrons q = 5 x 10^{-11} referring to [49], electron temperature T_e = 4,81 x 10^{-19} Joules which give rise to electron-ion collision frequency of ν_{ei} = 3,6 x 10^{16} Hz indicating a low conductive plasma property. Despite the fact that electron-ion collision frequency reveals conductivity property of a plasma, a more detailed investigation is required to calculate the exact value of conductivity to compare with the conductivity limit of σ = 2 x 10^{-11} S/m for the measurement.

3.9 Conductivity calculation

To calculate the exact value of conductivity one must first make an assumption if the plasma is highly or weakly ionized. Depending on the ionization rate of plasma, properties of plasma changes so are the mathematical definition of electron-ion collision frequency and formulas for calculation of conductivity. In this research, both assumptions are investigated. As an initial foresight, it can be stated, that a highly conductive plasma has higher conductivity compared to weakly ionized plasma due to the higher mobility of electrons in the absence of a magnetic field. Moreover, a further investigation must be done for a plasma under a magnetic field (anisotropy of conductivity) which is more of an interest in this research.

3.9.1 Conductivity of the fully ionized plasma

A fully ionized plasma illustrates a highly conductive medium with high mobility of electrons. High mobility refers to that electrons will move freely experiencing relatively fewer collisions with ions compared to weakly ionized plasmas. This will result in a lower level of electron-ion collisions so a higher conductivity. The conductivity of plasma has first appeared in the paper of Lyman Spitzer as plasma resistivity according to [50]

$$\eta = \frac{\sqrt{4\pi m} Z \mathrm{e}^2 \ln \Lambda}{(4\pi\epsilon_0)^2 (3T_e)^{3/2}} \tag{3-18}$$

$$\sigma = \frac{1}{\eta} \tag{3-19}$$

σ	*Conductivity (S/m)*
η	*Resistivity* ($\Omega.m$)
m	*Electron mass (kg)*
Z	*Ion charge number (-)*
e	*Charge number of electrons (C)*
$\ln \Lambda$	*Coulomb logarithm (-)*
ϵ_0	*Permittivity of free space (F/m)*
T_e	*Electron temperature (J)*

Assuming that ions in the plasma are singly charged Z =1, coulomb logarithm ln Λ = 10, and electron temperature T_e = 4,81 x 10^{-19} J, resistivity of plasma η = 4,05 x 10^{-5} Ω. m and so the conductivity results in σ = 2,46 x 10^4 S/m which is recognized as electrically conductive [49]. This level of conductivity is close to the electrical conductivity of highly conductive metals such as silver and copper as seen in Figure 3-18. On the other hand, materials which have electrical conductivity less than 10^{-8} S/cm are assumed to be insulators. As an example, glass, diamond and fused quartz can be given.

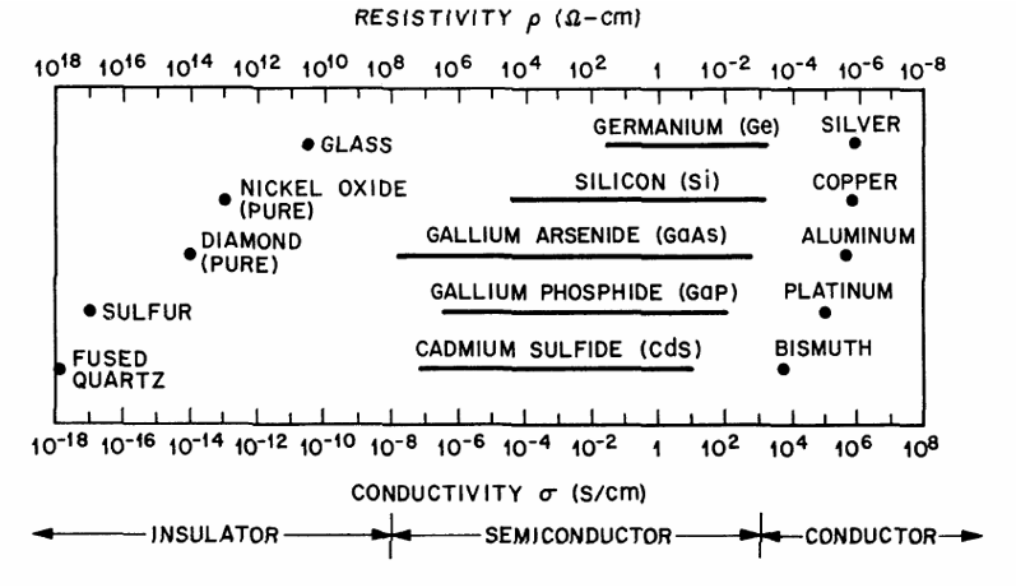

Figure 3-18: Electrical conductivity spectrum of materials [51]

Alternatively, the conductivity of fully ionized plasma can be calculated with conductivity formula derived from ohm's law below according to [52]

$$\sigma = \frac{n_e e^2}{m v_{ei}} \tag{3-20}$$

σ	*Conductivity (S/m)*
n_e	*Electron density (1/m³)*
e	*Electron charge (C)*
m	*Electron mass (kg)*
v_{ei}	*Electron ion collision frequency (Hz)*

Considering the fact that electron density, electron charge and electron mass are taken constant in this research only variable in this formula is the electron-ion collision frequency v_{ei} = 5,6 x 10^4 Hz. For fully ionized plasma resulting in a conductivity level of σ = 5,03 x 10^3 Hz according to formula (3-20). This value is slightly lower than the conductivity calculated with Spitzer's formula (3-18). However, the difference between is relatively small compared to the order of

magnitude (less than 10). For further calculations, the value of Spitzer conductivity will be used since Spitzer formula is specifically derived for fully ionized plasmas.

3.9.2 Conductivity of the partly ionized plasma

In a partly ionized plasma electron have less energy due to lower temperatures according to lower ionization rate. This results in a higher electron-ion collision frequency ν_{ei} = 3,6 x 10^{16} Hz according to formula (3-17) restricting the electron mobility and so the conductivity of plasma. Therefore, a lower level of conductivity is expected for partly ionized plasma. According to formula (3-20) a conductivity of σ = 7,76 x 10^{-9} S/m is obtained which is much smaller than the one calculated for the fully ionization assumption. This level of conductivity is much larger than the required minimum conductivity of 2 x 10^{-11} S/m and therefore still suitable for this application.

3.9.3 Conductivity of plasma under the magnetic field

Plasma, as mentioned before, is a gaseous mixture which includes the same amount of negative and positive charges which makes the mixture neutrally charged. Moreover, one can assume that charges are randomly distributed which leads to a homogenous state on a macroscopic scale. This manner of state makes plasma equally conductive in all directions. However, when an external magnetic field is applied to plasma anisotropy come into question. The Lorentz force which is required for separation of positive and negative charges for the measurement generates a not homogenous distribution of charges. This distribution results in variations of conductivity respect to the axis of particle velocity, magnetic field and potential difference. This phenomenon is called anisotropy of plasma conductivity. As conductivity refers to a significant threshold for this research anisotropy in conductivity must be carefully investigated.

Due to the fact that plasma conductivity under magnetic field is directional one must define conductivity as a tensor. For a magnetic field aligned with y-direction (see Figure 3-19) the tensor (3-21) is described as follows [53]

$$\sigma = \begin{pmatrix} \sigma_p & -\sigma_H & 0 \\ \sigma_H & \sigma_p & 0 \\ 0 & 0 & \sigma_{\parallel} \end{pmatrix} \tag{3-21}$$

When electron-ion collision ν_{ei} and electron cyclotron frequencies ω_{ge} are explicitly written as below

$$\sigma_p = \sigma \frac{\nu_{ei}^2}{\nu_{ei}^2 + \omega_{ge}^2} \tag{3-22}$$

$$\sigma_H = \sigma \frac{\omega_{ge}\nu_{ei}}{\nu_{ei}^2 + \omega_{ge}^2} \tag{3-23}$$

$$\sigma_{||} = \sigma = \frac{n_e \mathrm{e}^2}{m\nu_{ei}} \tag{3-24}$$

The element σ_p Pedersen conductivity (3-22) relates to the conductivity, which is related to the electric field carrying the Pedersen current and so the induced voltage (z-axis) can be seen in green in Figure 3-19. Pedersen conductivity is the measure which must be compared with the conductivity limit. Hall conductivity σ_H (3-23) carries the Hall current on the axis of sound wave (x-axis) both perpendicular to magnetic and electric fields in blue. Parallel conductivity $\sigma_{||}$ (3-24) determines the current which is parallel to the magnetic field (y-axis) in red and is equal to the conductivity in unmagnetized case (3-20).

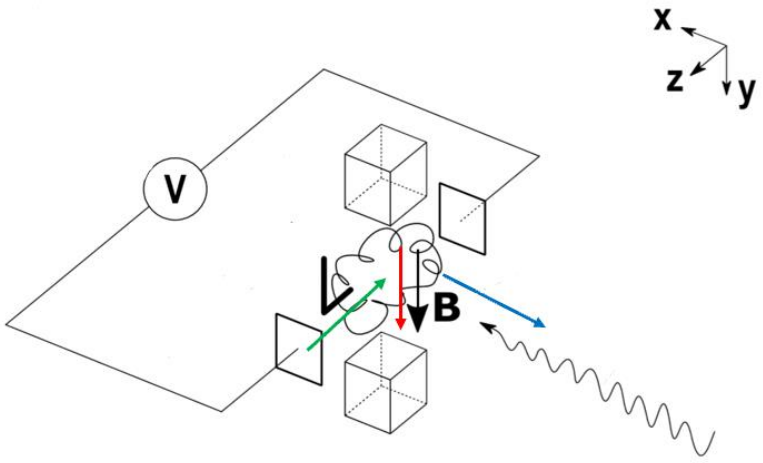

Figure 3-19: Anisotropy of conductivity on x, y, z axes [22]

Anisotropy characteristics of a plasma depend on the ionization rate of the plasma. Fully and weakly ionized plasmas show different properties when it comes to the anisotropy of conductivity. As it was discussed before for isotropic plasmas without external magnetic field the electron-ion collision frequency is the decisive parameter. If anisotropy is considered in case of a present external magnetic field, electron cyclotron frequency must be also taken into account in addition to electron-ion collision frequency. The ratio of both frequencies provides a base for a comparison between Pedersen, Hall and parallel conductivity.

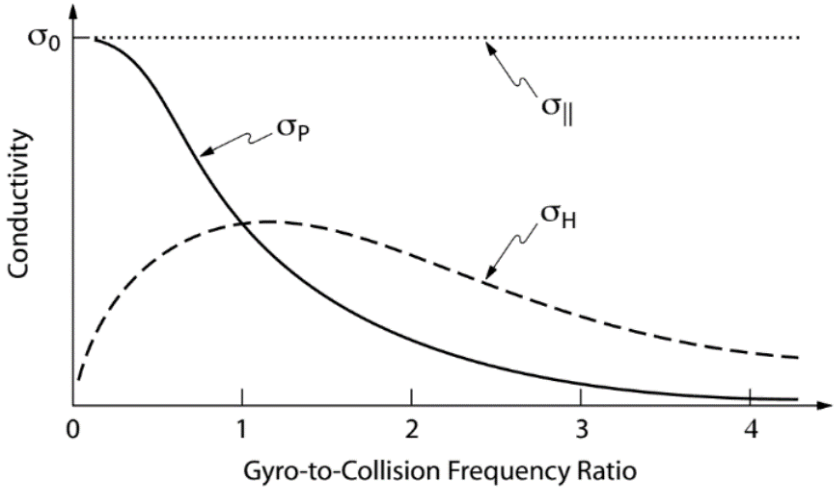

Figure 3-20: Gyro-to-collision frequency ratio respect to conductivity [52]

For a legit comparison let's assume that for both fully and partly ionized plasmas gyrofrequencies are the same. If the plasma is fully ionized, due to relatively low collision frequency gyro-to-collision frequency takes a very high number diverging to the end of the x-axis of the graph seen in Figure 3-20. Thus, for the assumption of a fully ionized plasma magnetic field has a negative effect on Pedersen conductivity.

	Fully ionized	Partly ionized
electron gyro(cyclotron) frequency(Hz)	5,64E+09	5,64E+09
electron ion collision frequency(Hz)	5,60E+04	3,63E+16
gyro-to-coliision frequency ratio(Hz)	1,01E+05	1,55E-07

Figure 3-21: Comparison of frequencies

This is an expected outcome as fully ionized plasmas are considered as diamagnetic [44]. If the plasma will be considered as fully ionized, an optimum value for magnetic flux density must be found. One has to avoid a decrease in Pedersen conductivity while keeping the magnetic field strong enough for generating enough induced voltage. This could be a further research topic as it illustrates a great complexity.

In the case of partly ionized plasma, the high electron-ion collision frequency rate gives rise to a very small gyro-to-collision frequency ratio can be seen in Figure 3-21. According to Figure 3-22, this illustrates no negative effect on Pedersen conductivity in this research. However, if stronger permanent magnets or magnet coils were used, magnetic flux density could be high enough to negatively influence the Pedersen conductivity. This property allows us to use ring permanent magnets as strong as possible to increase induced voltage without worrying about a decrease in Pedersen conductivity.

	Fully ionized	Partly ionized
plasma conductivity(S/m)	2,46E+04	7,76E-09
pedersen conductivity(S/m)	2,43E-06	7,76E-09
hall conductivity(S/m)	2,45E-01	1,20E-15
parallel conductivity(S/m)	2,46E+04	7,76E-09

Figure 3-22 : Comparison of conductivities

3.10 Magnetic field effects on plasma acoustics

In this research, plasma is exposed to a magnetic field for measurement purposes. The magnetic field allows a generation of induced voltage when plasma is excited by sound waves externally. On the other hand, the magnetic field has also influence on acoustic waves which are a topic of magnetoacoustics. In this chapter, the focus point will only be two magnetoacoustics phenomena.

3.10.1 Effect on the direction of the magnetic field

Firstly, deflection of magnetic field lines in a moving conducting fluid must be investigated since magnetic field strength perpendicular to the particle velocity is a crucial parameter for induced voltage. If the fluid is infinitely conductive, magnetic field lines are convected to follow fluid velocity field as there is strong coupling in between. Assuming that in plasma net charge is zero, from Maxwell's equations the relation between magnetic field, fluid velocity (in this application acoustic particle velocity) and conductivity can be derived according to [54] described in formula (3-25).

$$\frac{dB}{dt} = (B \cdot \nabla)u + \frac{c^2}{\sigma_p}\nabla^2 B \tag{3-25}$$

Where B is the magnetic field, u particle velocity, c phase velocity of particles, σ conductivity transverse to the magnetic field (Pedersen conductivity). For infinite conductivity, the second term vanishes as in formula (3-26).

$$\frac{dB}{dt} = (B \cdot \nabla)u \tag{3-26}$$

However, the conductivity attains a finite value in the case of weakly ionized gas in this application. Thus, the relation above for the finite conductivity must be also defined. If the conductivity is finite, the coupling between the magnetic field and moving conducting fluid is weaker. The magnetic field lines will not follow the fluid velocity field, but they will slightly shift through the conducting fluid. This shift must be quantitatively explained since it has a direct effect on the induced voltage. If magnetic field lines are perpendicular to particle velocity the expression can be formulated according to [54] seen in formula (3-27).

$$\frac{dB}{dt} = \frac{c^2}{\sigma_p}\nabla^2 B \tag{3-27}$$

In formula (3-27) can be seen that the first term existing in the formula for infinite conductivity vanishes which leads to a weaker coupling between the magnetic field and particle velocity. As the coupling decreases the angle between the magnetic field and particle velocity converges to normalized 90 degrees which are desired for the favour of induced voltage generation. To

investigate if the coupling and so the deflection of magnetic field lines with an angle ψ (seen in Figure 3-23) will occur in plasma, the following condition derived according to [54].

$$D_m = \frac{BL\sigma_p}{c^2\sqrt{\rho}} \gg 1 \tag{3-28}$$

D_m is the parameter for magnetic field-particle velocity coupling according to formula (3-28) B = 32,1 mT is magnetic field strength, L = 0,02 m is the length of plasma, σ_p = 7,76 x 10^9 S/m is Pedersen conductivity, c = 343 m/s is the speed of sound and ρ = 1,092 kg/m^3 is the density of air at T = 50 degree Celsius according to [55]. In this application the coupling parameter D_m = 4,05 x 10^{-17} which is well smaller than 1 making coupling of magnetic and particle velocity field negligible. As a result, the induced voltage can be calculated with the assumption of perpendicular magnetic and velocity field.

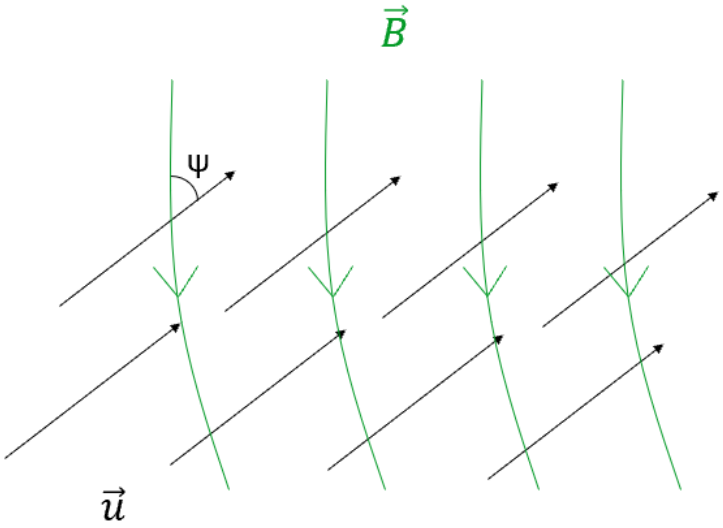

Figure 3-23: Deflection of magnetic field lines in a sound field

3.10.2 Effect on the speed of sound

Moreover, the magnetic field in plasma has an effect of phase velocity of charged particles. This effect only comes to a question when plasma length is not smaller than the acoustic wavelength scale. In this application, the size of the plasma is assumed to be smaller than the acoustic wavelength. However, if the voltage was not induced as expected level, a larger size of plasma up to a few cm must be used. In this case, the variation in speed of sound must be calculated. As a first estimation, an increase in phase velocity of sound is expected due to additional restoring force (Lorentz force) exerted on the particle in motion in the charged gas. This effect would increase with the degree of coupling between the magnetic field and velocity field. To define this effect quantitively the following formula of the dispersion relation is used [54].

$$c_p^2 = \left(\frac{\omega}{k}\right)^2 = c_s^2 + c_A^2 \frac{1}{1+\mathrm{i}\omega\tau_1(c_s k/\omega)^2} \tag{3-29}$$

Where c_p is the speed of sound in magnetized plasma, $\tau_1 = c^2/c_s^2\sigma_p$ as relaxation time of magnetic field lines, $c_s^2 = 1/\kappa\rho$ the speed of sound for zero conductivity, and $c_A^2 = B^2/\rho$ as the speed of sound along the magnetic field lines (Alfvén waves), ω as the angular velocity of propagating sound wave and k as the propagation constant. For the infinite conductivity, the phase velocity is $\omega/k = \sqrt[2]{c_s^2 + c_A^2}$ while $\omega\tau_1 = 0$. For zero conductivity which is the other limiting case, the phase velocity is equal to $\omega/k = c_s$. For finite conductivity, the propagation constant k is complex for real values of ω and through conductivity losses the sound wave is attenuated [54].

In this application, the magnetic flux density B has a low order of magnitude (order of mT). The conductivity is in order of nS/m which is close to air conductivity ($\sigma_{air} = 10^{-12}$ S/m) and a small number compared to the multiplication term $(c_s k/\omega)^2$. Thus, there will be no significant change in the second term in equation (3-29). In conclusion, the effect of magnetic field on the speed of sound in this particular application can be neglected.

3.11 Sound generation in plasma

In this application, plasma is subjected to acoustic waves externally. Therefore, stable and noise-free plasma is desired. In this context, the sound generated in plasma is investigated. In weakly ionized plasma neutral atom density dominates thus electrons and ions are forced to trace neutral air molecules when they are perturbated by a sound wave. According to this statement, the existence of charged particles seems insignificant for plasma acoustics. Nevertheless, some amount of energy is transferred to neutral gas from charged particles which draw energy from external electric fields. This transferred energy to neutral gas can give rise to sound generation and amplification in the weakly ionized plasma [54].

The energy transfer to neutral particles from electrons cause not only an increase of temperature of neutrals but also results in the creation of new charged particles. The process of creation of charged particles will travel as a wave through the plasma. This wave propagation is a different wave mode in which there is a charge separation apart from ordinary sound waves travelling in plasma. This kind of sound wave is widely called a plasma wave or plasma oscillation. The wave interaction and propagation under an external magnetic field is, however, more complicated which has to be investigated with aspects of magneto-acoustic waves in conducting fluid [54].

Assuming that initially there is no external magnetic field. Electrons attain higher temperatures about 10^4 to 10^5 K compared to much lower temperatures of neutrals about 330 K in a weakly ionized plasma. Due to this temperature difference energy flows from electrons to neutrals. If this energy transfer is made vary with the time, the sound will be generated in the plasma. The sound pressure existing in the plasma due to the energy transfer is described according to [54] in formula (3-30)

$$p_0 = 4(k-1)\frac{m_e}{m_\mathrm{n}}\frac{v_e}{c}\frac{L}{l_e}p_e \tag{3-30}$$

Where ratio of specific heats k = 1,4 , electron mass m_e= 9,11x10^{-31} kg, neutral mass m_n= 4,81x10^{-23} kg, average electron velocity v_e = 1000 m/s [54], speed of sound c = 361 m/s at 50 Celsius plasma temperature [56], plasma length L = 20 mm, average mean free path of electrons l_e = 2,75x10^{-14} m, and sound pressure of electrons p_e = 4,55x10^{-9} Pa. Consequently, a sound pressure of p_0 = 2,78x10^{-4} and sound pressure level of SPL = 23 dB is estimated in plasma due to internal sound generation. If we compare 23 dB with possible sound pressure level of excitations to be measured (from 60 dB), the sound generated due to plasma is barely audible and illustrates no problem for the operation of PPVS.

4 Design of measurement setup

In this chapter, parts which are used in the measurement setup are treated. As it is the most important part of the measurement setup, an appropriate choice of plasma generator is necessary for the realisation of the new measurement method. According to dimensions of plasma generator a permanent magnet is chosen. To generate acoustic waves for excitation of plasma a loudspeaker is used. Consequently, two electrodes and a voltage measurement unit are assembled to the system to detect the induced voltage.

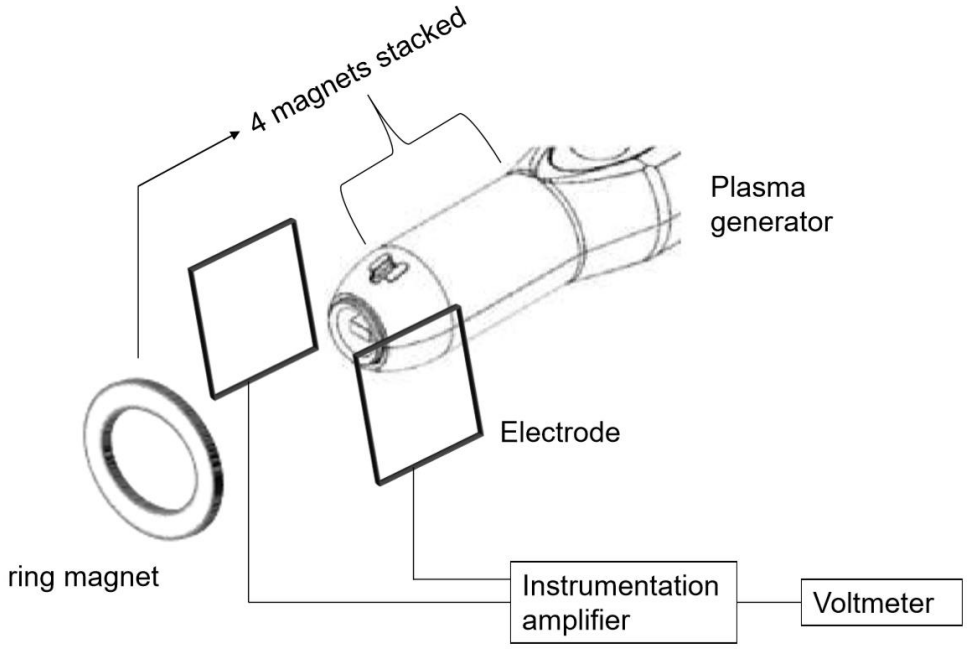

Figure 4-1: Measurement setup [59]

4.1 Plasma generator

As stated in chapter 3.1.4, the piezoelectric direct discharge (PDD) method was found to be useful for the application target. For this research, a plasma plume which has adjustable length and width is required for testing purposes. Therefore, a plasma device with flow feed is required. Piezobrush, a hand-held plasma generator, which is designed and developed by Relyon Plasma is taken for investigations and tests. The Piezobrush device has a piezoelectric transformer named as Ceraplas which has a high voltage output and generates a plasma. Ceraplas is a Rosen type piezoelectric transformer [57] based on a hard PZT (lead zirconate titanate) ceramic material, which can be co-fired with internal copper electrodes [58]. Rosen type piezo transformers have a high transformation ratio of voltage which makes them very suitable for cold plasma generation. An input voltage of 12V to 24V leads up to 15 kV of output voltage depending on the load. Specifications of Ceraplas device in Figure 4-1.

Operating voltage [V_{pp}]	12 to 24
Operating frequency [kHz]	~ 50
Output voltage [kV]	Up to 15 (depending on load)
Transferred power [W]	10 (max.)
Plasma temperature [°C]	<50
Processing gas	Air, industrial gases such as N2, Ar, He
Ozone generation rate [ppm] (at 8 W with customized measurement set up)	20
Dimensions [mm]	72 × 6 × 2.8
Material set	Hard PZT with co-fired copper electrodes
Assembly	Soldered mounts and connections at nodal points

Figure 4-2: Datasheet of Ceraplas device [58]

According to datasheet a plasma temperature of maximum 50 degree Celsius under 10 W transferred power is measured which makes Ceraplas suitable for hand-held operation. However, the Ceraplas device generates plasma on four corners of its output surface that generates a very weak and yet inhomogeneous ionization.

To overcome this hurdle, Piezobrush device was chosen for tests and investigation due to the fact that higher ionization rate allowing a more homogenous plasma. The Piezobrush (PZ2) device has a body around the driver for safe hand-held operation. Moreover, there are different nozzles provided for feed gas into plasma which is required for this research (see Figure 4-2).

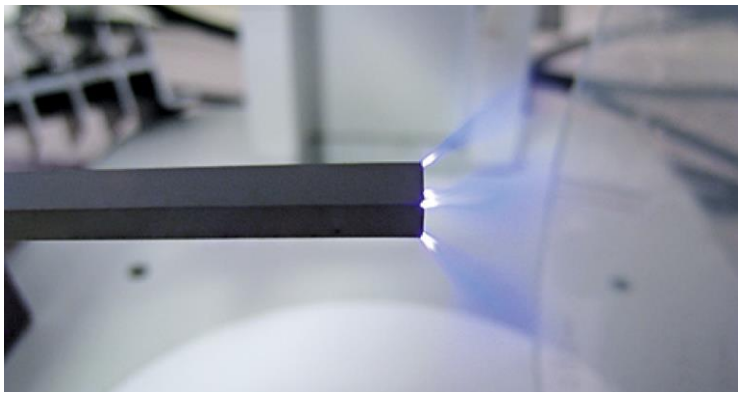

Figure 4-3 : Ceraplas in operation [58]

In this particular research, the air is fed by an internal axial fan through the hose. The nozzle has a diameter of 20 mm. Flow range is approximately 0.5 to 3.0 litres/minute [59]. Due to fan operation and additional electronics, PZ2 has a relatively higher power consumption of 30 W compared to 10 W consumption of Ceraplas driver alone. However, it still can be operated with 15 DC which allows a battery-powered operation allowing required mobility for particle velocity measurements. The width of plasma generated varies 5-20mm depends on process parameters such as voltage and gas supply seen in Figure 4-3. Temperature range for operation is between 10-40 Celsius illustrates reasonable limitation for particle velocity measurements indoors.

Figure 4-4 : Piezobrush in operation [59]

Electrical data	
• Supply voltage	15 V DC
• Power consumption	max. 30 W
• Model	Handheld device with external power plug
Dimensions	
• Weight	170 g (not including external power plug)
• Length	215 mm
• Diameter max.	36 mm
• Diameter min.	27 mm
• Cable length	1500 mm
Typical application parameters	
• Plasma temperature	< 50 °C
• Distance for treatment	2 – 10 mm
• Width of treatment	5 - 20 mm depending on process parameters
• Treatment speed	10 – 20 mm/s
Operating conditions	
• Air humidity	< 80% rel. (non-condensing)
• Temperature	10 – 40 °C; 50 – 104 °F
Storage conditions	
• Air humidity	< 80% rel. (non-condensing)
• Temperature	0 – 60 °C; 32 – 140 °F

Figure 4-5: Datasheet of Piezobrush [60]

Considering factors of safety, mobility and plasma generation Piezobrush is a convenient device for feasibility tests of particle velocity measurements.

4.2 Permanent ring magnet

To provide an axial magnetic field to plasma a permanent magnet is used. Specifications of the magnet have already been presented in chapter 3.2, as it was necessary to calculate exact magnetic flux density exerted on plasma. The magnet is stacked right above the gas hose of the nozzle indicated with arrows in Figure 4-5.

Figure 4-6: Permanent ring magnet [35]

The permanent magnet has an inner diameter of 9,5 mm, an outer diameter of 19,1 mm and a height of 6,4mm. It can operate at temperatures up to 80 degrees Celsius [35] which is well above the maximum temperature of 50 degrees Celsius for plasma.

4.3 Voltage detection unit

To detect the induced voltage signal following devices must be present in the measurement chain

- Measuring electrodes
- Instrumentation amplifier

Considering the nanovolt level induced voltage output each component mentioned above must be specifically chosen for this application. Among those electrodes and instrumentation amplifier selection is a more significant challenge than electronics will be used to perform calculations in order to obtain acoustic particle velocity from the induced voltage signal.

4.3.1 Measuring electrodes

For an electrode low noise level and high stability are the most important properties when used measuring nanovolt potential differences [61]. When measuring nanovolt potential difference significant errors may occur by offset voltages and noise sources which can mostly be neglected while measuring higher voltage levels. A voltmeter typically reads zero voltage, when it is connected to a relatively low impedance circuit when there is no voltage present. However, a

voltage can be read in voltmeter called “offset voltage” due to several error sources. These error sources are [62]

- Thermoelectric electromotive force (EMF)
- Rectification of radio frequency interference (RFI)
- Offsets in the voltmeter input circuit

Those errors can be explained with the following concepts below [62]

- Johnson noise
- Magnetic fields
- Ground loops

The most common and for this application important noise is Johnson or thermal noise. Johnson noise is the voltage related to the motion of electrons due to their thermal energy at temperatures above zero Kelvin [62]. Considering the fact that all voltage sources have internal resistance, Johnson noise is present also in the electric circuit used for this application. Johnson noise is determined according to the equation below [62]

$$V_n = \sqrt{4k_B T R \Delta f} \tag{4-1}$$

V_n	*Noise voltage developed in source resistance (V)*
k_B	*Boltzmann constant (J/K)*
T	*Absolute temperature of the source (K)*
R	*Source resistance (Ω)*
Δf	*Noise bandwidth (Hz)*

As seen in equation (4-1) temperature of the source has a significant effect on the noise generated. Although it is not possible to decrease the plasma temperature of 50 degrees Celsius, an electrode material with relatively low thermal conductivity can be chosen to keep electrodes as cool as possible. In this context, a copper electrode is more advantageous than a silver electrode thanks to its lower thermal conductivity seen in Figure 4-6. However, a more detailed investigation must be done as the electrical conductivity of the electrode is also a significant property of the measurement chain. This can be treated as a further research topic in the future.

(Metal 100)	Electrical Resistivity at 293 K, μΩcm	Thermal Conductivity $Wm^{-1}k^{-1}$	Relative Electrical Conductivity (Copper = 100)	Relative Thermal Conductivity (Copper = 100)
Silver	1.63	419	104	106
Copper	1.694	397	100	100
Gold	2.2	316	77	80
Aluminum	2.67	238	63	60

Figure 4-7: Electrical resistivity and thermal conductivity of copper and other commercial metals at 293K [64]

Magnetic field noise for this application can be neglected although there is a magnetic field in the circuit. The reason is that magnetic field noise is only relevant, if the field is changing with time, and if there is relative motion between the circuit and the field [62]. In this application, a stable permanent magnet provides a constant magnetic field. However, if a constantly changing magnetic field is applied to the circuit for signal post-processing purposes, this effect must be considered.

Ground loops form when both the voltage source and measurement instrument are both connected to a common ground bus as seen in Figure 4-6. In this application, the voltage source (experiment) to be detected is the induced voltage in plasma which is separately grounded. Therefore, this effect can also be neglected.

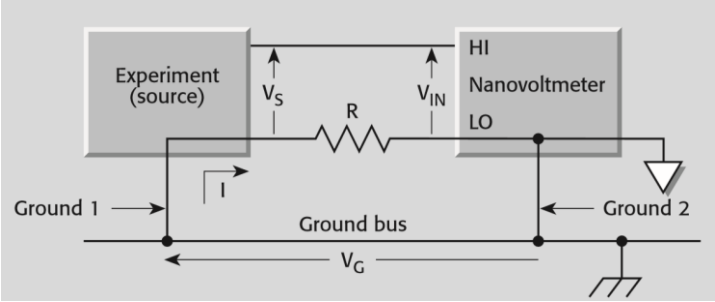

Figure 4-8: Ground loop [62]

V_s *Source voltage (V)*

V_{IN} *Input voltage for nano voltmeter (V)*

V_G *Ground loop interference voltage (V)*

R *Resistance of input LO connection (Ω)*

I *Current passing through input LO connection due to ground voltages in the ground bus (A)*

Consequently, the geometry of the electrodes has also an effect. Size of electrodes must be big enough to cover whole plasma plume which is around 20 x 20 mm^2. However, a slightly larger cross-section of the electrode of 30 x 30 mm^2 can be chosen to confine the plasma plume safely in all conditions regardless of changes i.e. wind or other disturbances.

4.3.2 Instrumentation amplifier

As it is mentioned in chapter 3.4 an instrumentation amplifier is a crucial part of the electronic circuit in this application. Due to the nanovolt level of the induced voltage signal, an instrumentation amplifier is required. AD8428 low-noise in-amp can be applied to the circuit to tackle difficulties to read nanovolt induced voltages in plasma. AD8428 provides a precise gain of 2000 with 5ppm/°C max gain drift, 0.3 µV/°C max offset voltage drift, 140 dB min CMRR to 60 Hz (120 dB min to 50 kHz), 130 dB min PSRR, and a 3.5 MHz bandwidth, the AD8428 is suitable for the circuit to detect voltages in order of nanovolts. Most significantly, the 1.3-nV/√Hz voltage noise at 1 kHz and the 40-nV p-p noise from 0.1 Hz to 10 Hz enable

high signal-to-noise ratio with very small signals. Moreover, two additional pins enable to change the gain or add a filter to reduce the noise bandwidth [65].

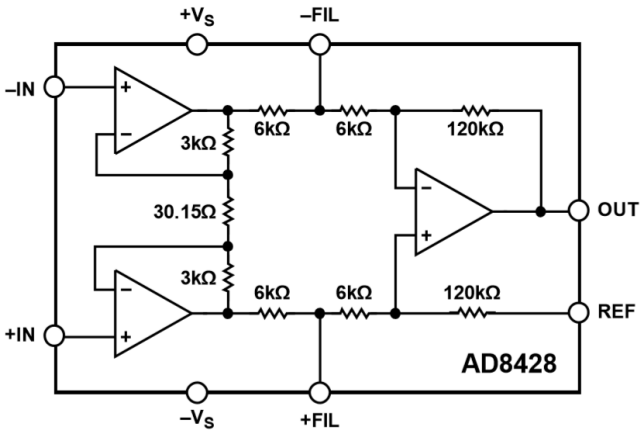

Figure 4-9: Functional block diagram of AD8428 [66]

5 Conclusion

The evaluation of the feasibility of plasma particle velocity sensor depends on the outcome of several investigations made in this research which is initially mentioned in chapter 2.2 briefly. Firstly, an estimation of expected induced voltage is calculated according to Faraday's formula of electromagnetic induction referring to the specifications of a typical permanent ring magnet. As a result of this investigation, it has been realized that an order of magnitude of nanovolts is to be expected as a potential difference. This potential difference leads to the application of high-end, high-accuracy instrumentation amplifier necessary for reliable voltage measurement. Moreover, to verify this voltage the concept of coherence spectrum analysis (coherence function) is introduced. To sum up, the effects of the induced voltage and its measurement illustrates no problem for the feasibility.

Secondly, the investigation of minimum conductivity required for this measurement has been done. A minimum conductivity limit of $\sigma = 2\,x\,10^{-11}$ S/m was found for voltage detection according to Kirchhoff's rule of closed-loop with a simple electronic circuit model. To compare this value with the actual conductivity, plasma conductivity has been calculated with plasma parameters determined by data obtained from a typical plasma generator device with piezoelectric direct discharge principle. Both fully and partly ionization assumptions delivering respectively a conductivity (Pedersen conductivity) of σ = 2,43 x 10^{-6} S/m and σ = 7,76 x 10^{-9} S/m which are well above the conductivity limit seen in Figure 5-1. Thanks to this comparison, the most significant challenge of making air enough electrically conductive is clarified. The air can be ionized with plasma generation sufficiently conductive for the feasibility.

	Fully ionized	Partly ionized	Limit
pedersen conductivity(S/m)	2,43E-06	7,76E-09	2E-11

Figure 5-1: Comparison of conductivities for feasibility

Moreover, magneto-acoustic effects are investigated. According to investigations done, no significant effect on the measurement is expected. Magnetic flux density is negligibly small to deflect the magnetic field lines and deviate the speed of sound in plasma. Moreover, the sound generated due to plasma is also at a negligible level of 23 dB. According to these investigations magneto-acoustic effects have no harm for the feasibility of this method.

Finally, a measurement setup with commercially available parts is presented. These parts comply with the following boundary conditions mentioned in chapter 3.

- Plasma generation method
- Induced voltage
- Electrical conductivity
- Magnetoacoustics
- Sound generation in plasma

Consequently, it can be stated that the detection of induced voltage to calculate acoustic particle velocity is possible. This is the proof that states the feasibility of the novel measurement method. According to the outcome of this thesis work, a practical work which includes the building of a physical experiment setup can be done. In this future work details of signal, post-processing can also be investigated as an interesting challenge.

6 References

[1] *"Sound Intensity"*, Brüel & Kjær, Revision September, 1993

[2] Comesaña, D.F. et al., *"Scan and Paint:Theory and Practice of a Sound Field Visualization Method"*, ISRN Mechanical Engineering, vol. 2013, Article ID 241958, 11 pages, 2013

[3] "*Sound Intensity Probe Nor1290"*, Norsonic, Retrieved June 2019,

https://web2.norsonic.com/product_single/sound-intensity-probe-nor1290

[4] Webster, J.G., "*Measurement Instrumentation and Sensors Handbook"*, CRC Press LLC, 1999

[5] Stornelli, V. et al., *"The assessment of wind conditions by means of hot wire sensors and a modifed Wheatstone bridge architecture"*, Sensors and Actuators A 262 130–139, 2017

[6] "*Hot wire anemometry"*, Retrieved June 2019,

https://www.jove.com/science-education/10464/hot-wire-anemometry

[7] "*Hot-film air-mass meter"*, Bosch, Retrieved June 2019,

https://www.bosch-mobility-solutions.com/en/products-and-services/passenger-cars-and-light-commercial-vehicles/powertrain-systems/sensors-for-the-powertrain/hotfilm-airflow-sensor/

[8] H-E de Bree., "*The Microflown: An acoustic particle velocity sensor"*, Sensors and Actuators A 69 126-133, 1998

[9] de Bree, H.E. et al., "*Experiments with a new acoustic particle velocity sensor in an impedance tube",* Sensors and Actuators A 69 126-133, 1998

[10] *"Sensors&Probes"*, Microflown, Retrieved June 2019,

https://www.microflown.com/products/standard-probes/u-regular/

[11] Mayinger, F., Feldmann, O., *"Optical Measurements: Techniques and Applications"*, Second corrected and revised edition, Springer, 2000

[12] Le Duff, A. et al. *"Acoustic velocity measurements in the air by means of laser doppler velocimetry: Cramer-Rao bounds and maximum likelihood approximation"*, 1988

[13] Valiere, J.C. et al., *"Acoustic velocity measurements in the air by means of Laser Doppler Anemometry: Dynamic and frequency range limitations and signal processing improvements"*, IEEE International Conference, Volume 2, 2002

[14] Hann, D.B, Greated, C.A., *"The measurement of flow velocity and acoustic particle velocity using particle-image velocimetry"*, 1997

[15] Tonddast-Navæi, A., *"Acoustic Particle-Image Velocimetry: development and applications",* PhD thesis The Open University, 2005

[16] Johnson, R.W. et al., "Processes and Procedures for Application of CFD to Nuclear Reactor Safety Analysis", September 2006

[17] Eren, H., Liptak, B.G., Kopp, H.G., *"Magnetic Flowmeters",* Instrument Engineers Handbook, CRC Taylor&Francis, 2003

[18] Gangl, G. et al., *"Influence of Measurement Inaccuracies at a Storage Tank on Water Losses"* IWA Water Loss Conference, Conference Proceedings, Volume II, 2007

[19] *"Magnetic Flowmeter Fundamentals",* Rosemount Measurement, 1995

[20] Béquin, P. et al*., "Corona Discharge Velocimeter",* Acta Acustica united with Acustica, Hirzel Verlag, 104 (3), pp.477 - 485, 2018

[21] Venkatramani, N., *"Industrial plasma torches and applications"*, Current Science, Vol. 83, No. 3, pp. 254-262, 2002

[22] Fuchs, A., Patent application: *"Method and Device to Determine Acoustic Gas Particle Velocity"*, Virtual Vehicle Research GmbH, 2018

[23] *"Lorentz Force"*, Retrieved July 2019,

https://de.wikipedia.org/wiki/Lorentzkraft

[24] Hartmann, P. et al., *"Strongly Coupled Plasma Liquids"*, 2007

[25] *W. Siemens. Poggendorffs Ann. Phys. Chem. 102, 66 (1857)*

[26] Yan, W., Economou, D. J., *"Gas flow rate dependence of the discharge characteristics of a helium atmospheric pressure plasma jet interacting with a substrate"*, Journal of Physics D: Applied Physics, 2017

[27] Hoffmann, C. et al., *"Cold Atmospheric Plasma: methods of production and application in dentistry and oncology"*, Medical Gas Research, 2013

[28] *"Dielectric Material as an Electric Field Medium",* Retrieved September 2019,

https://www.electrical4u.com/dielectric-material-as-an-electric-field-medium/

[29] Valinčius et al., *"Report on the different Plasma Modules for Pollution Removal MO 03"*

[30] Ebert, U. et al., *"Structure formation in a DC-driven barrier discharge: stability analysis and numerical solutions"*, 28th ICPIG, 2007

[31] Kogelschatz, U., *"Fundamentals and applications of dielectric-barrier discharges"*, 2000

[32] Carazo, A.V., *"50 Years of Piezoelectric Transformers. Trends In The Technology"*, 2011

[33] Teschke, M., *"Piezoelectric Low Voltage Atmospheric Pressure Plasma Sources"*, 2009

[34] *"Cold plasma from a single component"*, Retrieved September 2019,

https://www.tdk-electronics.tdk.com/en/373562/tech-library/articles/applications---cases/applications---cases/cold-plasma-from-a-single-component/1109546

[35] *"Ringmagnet Ø 40.0 x 25.0 x 5.0 mm N42 Nickel"*, Retrieved September 2019,

https://www.magnet-shop.com/neodymium/ringmagnets/ringmagnet-40.0-x-25.0-x-5.0-mm-n42-nickel-holds-8-kg#

[36] *"Formula for ring magnet flux density"*, Retrieved September 2019,

https://www.supermagnete.de/eng/faq/How-do-you-calculate-the-magnetic-flux-density

[37] *"Introduction to Operational Amplifiers (Op-amps)"*, Retrieved November 2019,

https://www.allaboutcircuits.com/textbook/semiconductors/chpt-8/introduction-operational-amplifiers/

[38] Kitchin, C., Counts, L., *"A Designer's Guide to Instrumentation Amplifiers"*, second edition, 2004

[39] Golińska, A.K., *"Coherence function in biomedical signal processing: a short review of applications in Neurology, Cardiology and Gynaecology"*, 2011

[40] Scharrer, R., Vorländer, M., *"Sound Field Classification in Small Microphone Arrays Using Spatial Coherences"*, IEEE Transactions on Audio, Speech, and Language Processing, Volume: 21 , Issue: 9 , 2013

[41] P. D. Welch, *"The use of fast Fourier transform for the estimation of power spectra:A method based on time averaging over short, modified periodograms"*, IEEE Trans. Audio Electroacoust., vol. AU-15, no. 2, pp. 70–73, 1967

[42] S.L.Marple, *"Digital Spectral Analysis With Applications"*, Englewood Cliffs, NJ, USA:Prentice-Hall, vol.1, p.512, 1987

[43] *"Conductivity",* Retrieved November 2019,

http://maxwells-equations.com/materials/conductivity.php

[44] Chen, F.F., *"Introduction to plasma physics and controlled fusion. Second edition"*, Plenum Press, 1984

[45] Nettesheim, S. et al., *"Effect of piezoelectric direct discharge plasma on microorganisms"*, 2015

[46] *"Plasma resistivity",* Retrieved November 2019

http://plasma.physics.swarthmore.edu/brownpapers/resistivity.pdf

[47] Fortov, V.E. et al., *"Physics of strongly coupled plasma"*, Clarendon Press, 2006

[48] Wiesemann, K., *"A short introduction to plasma physics"*, CERN Yellow Report, pp.85-122, 2013

[49] *"Plasma Physics 1"*, Retrieved November 2019,

http://sites.apam.columbia.edu/courses/apph6101x/Plasma1-Lecture-6.pdf

[50] Spitzer, L., *"Physics of Fully Ionized Gases"*, New York: Interscience (2nd edition), 1962

[51] *"Electrical Conductor"*, Retrieved December 2019,

https://www.britannica.com/science/electrical-conductor

[52] Piel, A., *"Plasma Physics: An Introduction to Laboratory, Space, and Fusion Plasmas Second Edition"*, Springer, 2017

[53] Baumjohann, W., Treumann, R., *"Basic space plasma physics revised edition"*, Imperial College Press, 2012

[54] Morse, P.M.&Ingard, K.U., Theoretical Acoustics, McGraw-Hill, 1987

[55] *"Properties of air at 1 atm pressure"*, Retrieved September 2019

https://www.me.psu.edu/cimbala/me433/Links/Table_A_9_CC_Properties_of_Air.pdf

[56] Zuckerwar, A.J., *"Handbook the of Speed of Sound in Real Gases"*, Academic Press, 2002

[57] Rosen, C.A. et al., 1958 US Patent No 2830274

[58] *"Piezobrush®PZ2 plasma handheld device"*, Retrieved May 2019,

https://www.relyon-plasma.com/relyon-plasma-products/piezobrush-pz2/?lang=en

[59] *"Operating instructions for piezobrush®PZ2 nozzle inserts"*, Retrieved May 2019,

https://www.relyon-plasma.com/wp-content/uploads/2018/11/F0351602_BA_Düsen_PZ2_multilingual.pdf

[60] *"Operating instructions for Piezobrush® PZ2 handheld device"*, Retrieved May 2019,

https://www.relyon-plasma.com/wp-content/uploads/2018/10/F0351301_BA_piezobrush_PZ2_ML.pdf

[61] Rostami, B. et al., *"Design and Fabrication of an Ultra-low Noise Ag-AgCl Electrode"*, 2019

[62] *"Low Level Measurements Handbook"*, Keithley, Sixth Edition

[63] *"Seebeck Effect"*, Retrieved December 2019,

https://www.britannica.com/science/Seebeck-effect

[64] Brandes, E. A., *"Smithells Metals Reference Book"*, Sixth Edition, Butterworth Inc., 1983

[65] Gerstenhaber, M. et al., *"No Pain, High Gain: Building a Low-Noise Instrumentation Amplifier with Nanovolt Sensitivity"*, Analog Dialogue 49-05, May 2015

[66] *"Low Noise, Low Gain Drift, G = 2000 Instrumentation Amplifier"*, Retrieved January 2020, https://www.analog.com/media/en/technical-documentation/data-sheets/AD8428.PDF

7 List of Figures